Available online at www.sciencedirect.com
ScienceDirect
ATE 00 (2026) 1–35
ATE

Towards reliable model validation of evaporative coolers: Unified terminology and benchmark datasets

Alanis Zeoli[a,], Samuel Gendebien[a], Titouan Janod[a], Tala Moussa[b], Chadi Maalouf[b], Anna Pacak[c], Vincent Lemort[a],

[a] *Laboratory of Applied Thermodynamics, Aerospace and Mechanical Engineering Department, University of Liège, Allée de la Découverte 17, 4000 Liège, Belgium*
[b] *Institut de Thermique, Mécanique et Matériaux, Université de Reims Champagne-Ardenne, Campus du Moulin de la Housse 1039, 51687 Reims, France*
[c] *Department of Cryogenics and Aviation Engineering, Faculty of Mechanical Power and Engineering, Wrocław University of Science and Technology, Wybrzeże Wyspiańskiego 27, 50-370 Wrocław, Poland*

Abstract

Evaporative cooling technologies are getting more attention in the scientific community due to the urgent need to satisfy the growing demand for cooling buildings while decreasing CO_2 emissions. Evaporative coolers offer a promising alternative to standard vapour-compression cycles, and many evaporative cooler variants have emerged in recent years to improve their performance. Similarly, the number of models developed to assess the performance of evaporative cooler configurations and simulate their behaviour under various operating conditions is constantly increasing. To obtain relevant results using simulation, it is necessary to perform a proper model validation, which is often handled using experimental data from the literature. However, model validation based on data from the literature can be time-consuming because the terminology of evaporative cooler configurations is not unified throughout the literature, and it requires gathering data from existing papers, which is rarely accessible in tables. This paper provides a framework for model validation using a two-step approach. First, the authors propose a comprehensive classification of evaporative coolers to unify the denominations of evaporative cooler configurations and understand the advantages and drawbacks of existing configurations. Second, standardised datasets are provided for each identified type of evaporative cooler. 18 datasets have been generated using existing experimental and numerical data from the literature, covering various operating conditions. Full datasets are available in an online open-source database to help the reader with model validation of various evaporative cooler configurations.

Keywords: Evaporative cooling, Adiabatic cooling, Dew point cooling, Alternative air conditioning, Sustainable cooling, Model validation, Dataset

1. Introduction

1.1. Context

Indoor air conditioning is of significant importance for people's health and thermal comfort [1, 2], consequently representing a substantial portion of primary energy consumption worldwide. According to the International Energy

Email address: alanis.zeoli@uliege.be (Alanis Zeoli)

Nomenclature

A_a	Interface area for heat transfer in the evaporative cooler (m^2)
A_c	Cross-sectional area (m^2)
c_p	Specific heat capacity (J/kg K)
D_h	Hydraulic diameter (m)
e	Pipe effective roughness height (m)
f	Friction factor
H	Evaporative cooler height (m)
h_{ch}	Channel height (mm)
h_D	Convective mass transfer coefficient (kg/m^2s)
h_T	Convective heat transfer coefficient (W/m^2K)
i	Specific enthalpy (J/kg)
k	Conduction heat transfer coefficient (W/m K)
Le	Lewis number
$\dot{m}$	Mass flow rate (kg/s)
nb_{ch}	Number of channels
Nu	Nusselt number
P	Channel wetted perimeter (m)
Pr	Prandtl number
Re	Reynolds number
RH	Relative humidity
SPR	Secondary-to-primary airflow ratio
T	Temperature (K)
t_{wall}	Wall thickness (m)
$\dot{V}$	Volumetric flow rate (L/h)
v	Fluid velocity (m/s)
W	Channel width (m)
W^*	Effective channel width (m)
WWR	Effective to actual channel width ratio
x	Space coordinate

Greek symbols

ε	Effectiveness
ν	Kinematic viscosity (m^2/s)
σ	Wettability factor
ω	Humidity ratio (kg/kg)

Subscripts

d	Dry channel
dp	Dew point
i	Inlet
o	Outlet
p	Primary channel
pd	Primary dry channel
pw	Primary wet channel
s	Secondary channel
sd	Secondary dry channel
sw	Secondary wet channel
w	Wet channel
wb	Wet bulb
wf	Water film

Abbreviations

CF	Counterflow
DEC	Direct evaporative cooler
D-IEC	Dew point IEC
EB	Energy balance
EC	Evaporative cooler
ECT	Evaporative cooling technology
HEX	Heat exchanger
IEA	International Energy Agency
IEC	Indirect evaporative cooler
M-IEC	Maisotsenko-based IEC
XF	Crossflow

Agency (IEA) [3], the growth in space cooling demand is a global concern regarding energy management. If not addressed properly, the energy demand for air conditioners will triple by 2050.

Evaporative cooling technologies (ECT) offer a less energy-consuming and more environmentally friendly alternative to standard air conditioning techniques based on vapour compression, as they use the latent heat of vaporisation of water to refrigerate the air [4, 5]. Evaporative coolers (EC) are heat exchangers in which an evaporative cooling process occurs. Evaporative cooling relies on heat and mass transfer between air and water. It is a natural process during which water evaporates by absorbing energy from the surrounding environment. This heat transfer results in the cooling of the surrounding air. The main advantage of ECTs compared to traditional vapour compression systems is that they do not require synthetic refrigerant, which can contribute to global warming due to leakage in the atmosphere [6]. Moreover, since ECTs do not rely on an outdoor unit rejecting heat to the atmosphere, they do not contribute to the increase of the urban heat island effect [7].

The two main types of evaporative coolers are direct (DEC) and indirect (IEC). A DEC cools the air through moisture addition, whereas an IEC produces cold air without humidifying it [8]. As a result, IECs are particularly well-suited for a wide variety of applications [9–11], such as residential and office buildings space [12–16], industries [17],

data centres [18–21], agricultural storage and livestock air-conditioning [22, 23], greenhouses [24], pharmaceutics [25], and desalination processes [26, 27].

1.2. Identification of the problematic

In recent years, many variations of IECs have been proposed to improve the performance of evaporative coolers [28]. Countless literature reviews on evaporative cooling have been published, providing an overview of existing evaporative coolers, their operation, and their performance. A detailed literature review of those review works was performed to identify research gaps in understanding evaporative coolers. A summary of the most relevant review works, in relation to the present work, is provided in Table 1. The table emphasises how the present paper differs from existing literature reviews by highlighting the scope of each review paper. The main findings of the literature review are summarised hereafter.

- The most striking observation is the lack of standardisation amongst the denominations of evaporative cooler variants. For example, *M-cycle* can refer to four variations of the indirect evaporative coolers [10, 29].
- Most review papers present the working principles of the studied ECs in a psychrometric diagram. However, some representations are incorrect or incomplete. For example, the evolution of air conditions in the wet channels of the IEC often follows an iso-wet bulb, neglecting the sensible heat absorbed by the secondary air. Similarly, the evolution of air conditions in perforated IECs is often unclear and does not help in understanding the physical processes occurring in the evaporative cooler [30–33].
- There is no universally adopted classification of evaporative coolers, and none of the existing classifications includes all existing IEC variations.
- Several papers compare experimental results obtained in the literature in terms of tested operating conditions, geometrical characteristics, wet bulb and dew point efficiency, or even cooling capacity [6, 31–33]. However, none of them attempted to standardise the data found in the literature to make it more accessible for further research purposes.
- Caruana et al. [34] provided a comprehensive description of the models developed to predict the behaviour and performance of indirect evaporative coolers and their main variation, the dew point indirect evaporative coolers (D-IEC), and highlighted current limits and possible future developments in the field. In particular, they reported that 63% of the models were validated using numerical (3%) or experimental (60%) data from the literature, 26% were validated using experimental data from the authors, and 11% were not validated against data.
- Some papers review the existing numerical models and their implementation [31, 32], but the validation of those models is rarely addressed.
- For models of IEC variations, validation is generally performed only for the D-IEC configuration, and the validity for other configurations is assumed without further verification [35, 36].

1.3. Objective

This work is part of the activities of the Annex 85 project launched in 2020 by the IEA on indirect evaporative cooling technologies. The objective is to organise the literature on the classification of evaporative exchangers and compile experimental and numerical data for model validation.

The first objective of this paper is to review the existing EC configurations and propose a vertical classification of evaporative exchangers. A schematic representation of the evolution of the air conditions inside the exchanger is provided in a psychrometric diagram, and the strengths and limitations of each configuration are identified. The ECs have been divided into categories depending on their channel characteristics. Then, the categories are further divided depending on the most common configuration modifications proposed in the literature.

Reference	[9]	[6]	[30]	[31]	[34]	[37]	[32]	[33]	Present work
Year	2016	2021	2021	2022	2023	2023	2024	2025	2025
EC review									
Number of EC configurations	4	1	4	5	2	4	3	3	7
Working principle	✓	✓	✓	✓		✓	✓	✓	✓
Applications	✓		✓	✓		✓	✓	✓	✓
Classification								✓	✓
Experimental data									
Operating conditions		✓	✓	✓			✓	✓	✓
Summary of performance		✓		✓		✓	✓	✓	✓
Uniformisation of datasets									✓
Numerical modeling									
Comparison of numerical models			✓	✓	✓		✓		
Model parameters			✓			✓	✓		✓
Discussion on model validation					✓				✓

Table 1: Scope of previous review works about evaporative cooling devices.

The second objective of this paper is to develop an online collaborative database to provide experimental and/or numerical studies that can be used for model validation of various EC configurations. Since validation based on experimental data from the literature is a common practice, the authors found it useful to review the literature to identify the most suitable data for validating each EC configuration. Datasets were assembled by collecting data from the corresponding papers, following similar templates to standardise the data presentation and the provided variables using the nomenclature presented in this paper. All datasets can be found in an open-source database designed to be collaborative and constantly updated.

1.4. Structure of the paper

The paper is organised as follows. Section 2 reviews the EC configurations, outlines the classification proposed by the authors and discusses the performance evaluation of evaporative coolers. Section 3 introduces the methodology applied to obtain uniform datasets. Section 4 presents the 18 datasets selected for EC model validation. The datasets are further discussed in Section 5, which also provides insight regarding the future datasets that would be worth adding to the online database.

2. Theory of evaporative coolers

In this section, a new classification of the most common evaporative cooler configurations is proposed, laying the basis for the physical analysis of each EC configuration. The vertical classification of evaporative coolers is established in Section 2.1. Section 2.2 gives the nomenclature used in this paper for each EC configuration. Section 2.3 defines the main characteristics of the EC channels and introduces three main categories of evaporative coolers. Section 2.4 reviews the most common evaporative cooler configurations proposed in the literature. The interest of each variation is discussed using a psychrometric diagram to represent the evolution of air conditions in the evaporative cooler. Finally, Section 2.5 provides information on the performance evaluation of evaporative coolers, starting by defining the wet bulb and dew point efficiencies used in the literature. The applicability of these indicators to each identified evaporative cooler configuration is discussed.

2.1. Proposed classification of evaporative coolers

The first step of the uniformisation of the literature is the establishment of a general classification of evaporative coolers. A summary of the existing EC classifications is presented in Table 2. The existing classifications divide the

Num.	Refs.	Classification criteria	Identified configurations	Comment
1	[38], [39]	Evaporation strategy	Identification of 3 categories: DEC, IEC, and two-stage EC	Broad classification, suitable for a general identification of evaporative cooling categories.
2	[40], [41], [42]	General classification based on 1 but identification of sub-categories	Active and passive DEC, IEC/D-IEC, two-stage EC	Not all configurations included in sub-categories.
3	[33]	IEC system configuration and geometry	DEC, IEC, D-IEC, two-stage IEC-DEC	Classification of IEC technologies. Geometries are applicable to all IEC configurations.
4	[10]	Mix of classifications 1 and 3	DEC, IEC, D-IEC and M-IEC, two-stage EC and hybrid systems	Missing perforated versions of D-IEC and M-IEC. Geometries are applicable to all IEC configurations. Geometric characteristics can also be important for DEC.
5	Present work	Establishment of general EC categories, identification characteristics to differentiate configurations and proposition of an arborescence of evaporative coolers.	DEC, IEC, D-IEC, M-IEC perforated versions, two-stage EC.	Include all identified EC configurations regarding operational variants. Geometries were not introduced as they should be part of a different classification, and they influence the performance of the EC but not its physical principle of operation.

Table 2: Review of existing classifications and their use in the literature.

evaporative coolers into three main categories based on evaporation strategy: DEC, IEC and two-stage EC (including combinations of different ECs). In general, the variants of the IEC (conventional IEC, D-IEC and M-IEC) are simply identified as sub-categories of the IEC, while perforated D-IEC and M-IEC are not included in any existing classification. Some classifications also include different IEC geometries, although they generally apply to all IEC variations and should therefore be part of a different classification.

The classifications of evaporative coolers existing in the literature have been supplemented to create a new classification aiming to provide insights into the configuration design of evaporative coolers and the associated limitations (Figure 1). It lays the basis for understanding the differences between the configuration models proposed in the literature. All the EC variants introduced in the classification are detailed in Section 2.4.

The basic skeleton of the vertical classification proposed by the authors remains based on the evaporation process, resulting in three main evaporative cooler classes: direct evaporative coolers, indirect evaporative coolers and two-stage evaporative coolers. A DEC model contains wet channels only, while the IEC model requires the addition of dry channels. The two-stage EC models combine models of DEC and IEC, depending on the configuration.

The novelty of the proposed configuration lies in the sub-classification of the indirect evaporative coolers, which demonstrates the connections between the IEC variations and highlights the required model modifications. As identified in the previous section, several variations of the IEC have been proposed to increase performance. The D-IEC recirculates part of the primary air to be used as secondary air, which can be translated into a modification of the boundary conditions of the IEC model. The D-IEC can then be divided into two sub-categories: the perforated D-IEC and the M-IEC. The perforated D-IEC requires the inclusion of mass and energy conservation equations at the mixing point, while M-IEC requires the introduction of an additional dry channel for the secondary air. Finally, the physical principles of the perforated D-IEC and the M-IEC can be combined to form a new IEC variant, which is called the perforated M-IEC, with perforations between the secondary wet and dry channels.

It should be noted that other considerations can impact the modelling or performance of EC models, even though they have not been deemed relevant as key characteristics for this classification. For example, all configurations can be derived in cross or counterflow arrangements. Materials and possible plate corrugations are also important for the evaporative cooler performance [39, 43]. However, they have not been considered in the classification method, as they are not specific to one particular configuration. They are further discussed in Section 3.

2.2. *Unified terminology*

The nomenclature of evaporative coolers proposed in this paper is presented in Table 3. The table also lists the most common denominations found in the literature for each EC variant, along with their associated abbreviations. For most EC configurations, the selected denomination is the most popular in the literature. For example, direct evaporative cooler (DEC), indirect evaporative cooler (IEC), dew point IEC (D-IEC), and two-stage EC are common terms in the literature. Overall, the denominations have been selected to stay close to what is found in the literature, while being intuitive, except for the M-IEC. In M-IEC, the *M* stands for *Maisotstenko*, who has filed a patent for the M-IEC configuration. In the literature, the most common term for this configuration is *M-cycle*. However, M-cycle is also commonly used to refer to D-IEC, perforated D-IEC, M-IEC or perforated M-IEC, depending on the research team. In this paper, the name M-IEC has been selected for the 3-channel IEC (without perforations) for the following reasons:

- The D-IEC configuration was first introduced by Hsu et al. [44] (under the term *closed-loop IEC*) and thus cannot be attributed to Dr Maistsenko.
- The perforated D-IEC has characteristics similar to a D-IEC, but with perforations. The term D-IEC has been kept to highlight their similarity.
- Similarly to the perforated D-IEC, the term *perforated M-IEC* has been associated with the perforated variant of the M-IEC.
- The term ”cycle” can be confusing when referring to a component.

2.3. *Definition of channel characteristics*

The evaporative coolers are made of successive layers of channels. To better understand the physics of evaporative coolers, four channel features have been identified. They are defined below and summarised in Table 4.

- Primary channel (p): channel containing the *cooled fluid*. In the literature [32], it is also referred to as the *product* channel.
- Secondary channel (s): channel containing the *cooling fluid*. In the literature [32], it is also referred to as the *working* channel.
- Dry channel (d): channel in which the fluid exchanges *sensible heat*.
- Wet channel (w): channel containing air and water, in which water evaporation occurs, resulting in both *heat and mass transfer*.

Three EC categories can be defined based on the number of different channels within the exchanger, combining fluid type and transfer process (Table 5): direct (DEC), indirect (IEC), and Maisotsenko-based (M-IEC). They are detailed in the next section.

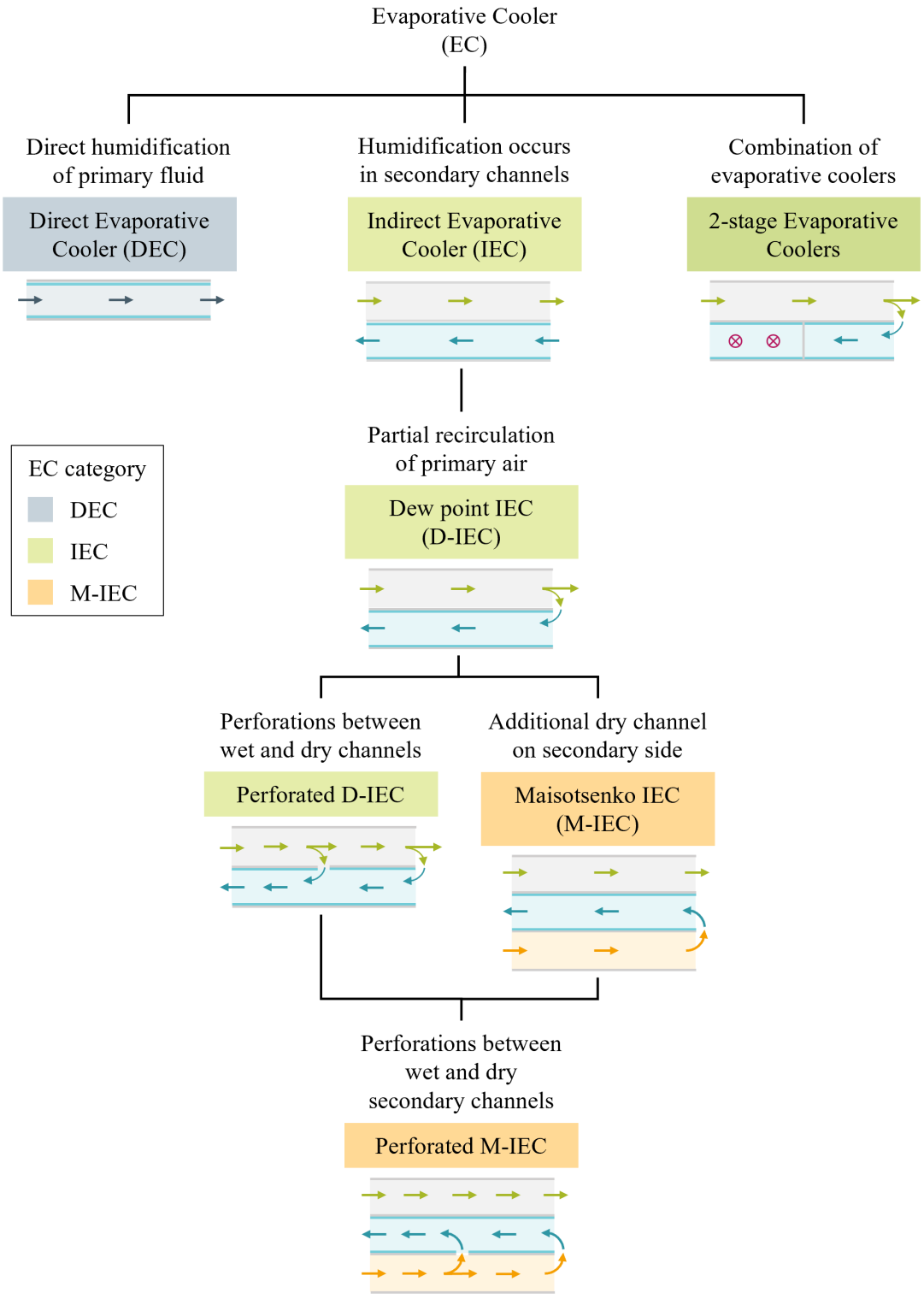

Figure 1: Classification tree of evaporative coolers.

Proposed nomenclature	Justification	Common denominations in the literature	Ref.
Direct evaporative cooler (DEC)	Most common denomination in the literature.	Direct evaporative pad (DEP)	[45]
	Gives a good insight into the physical process of the component.	Air-mediated direct evaporative cooling (AMDEC)	[46]
Indirect evaporative cooler (IEC)	Most common denomination in the literature.	Conventional IEC	[47]
		Wet bulb temperature IEC	[40]
	By opposition to *direct* evaporative cooling.	Air-mediated indirect evaporative cooling (AMIEC)	[46]
Dew point IEC (D-IEC)	Common denomination in the literature.	Dew point IEC (DIEC, DPIEC, DPEC)	[6, 32, 34, 48]
	Highlights the theoretical limit of the component.	Regenerative IEC (R-IEC, RIEC, R-D-IEC)	[10, 30, 33]
		Closed-loop IEC	[44]
		M-cycle	[29]
		Old M-cycle	[9]
		Sub wet bulb IEC	[40]
Perforated D-IEC	Same working principle as D-IEC but with perforation between dry and wet channels.	Muli-stage M-IEC	[47]
		M-cycle cooler	[29, 30]
Maisotsenko IEC (M-IEC)	In honour of the inventor of this configuration and its variants.	M-cycle (MEC)	[9, 29, 49]
		Dew point IEC	[33]
Perforated M-IEC	Same working principle as D-IEC but with perforation between dry and wet channels on secondary side.	M-cycle	[10, 29]
Two-stage EC	Most common denomination in the literature.	Multi-zonal IEC	[10]
		Combined EC	[50]
		Multi-stage D-IEC	[51]

Table 3: Proposed nomenclature for the EC technologies and summary of other common denominations for each EC variant.

Channel type	Abbreviation	Characterisation	Definition
Primary	p	Fluid type	Cooled fluid
Secondary	s	Fluid type	Cooling fluid
Dry	d	Transfer process	Sensible heat
Wet	w	Transfer process	Heat and mass

Table 4: Definition of the channel features.

	Fluid type	**DEC**	**IEC**	**M-IEC**
Channel 1	Primary	Wet (pw)	Dry (pd)	Dry (pd)
Channel 2	Secondary	/	Wet (sw)	Wet (sw)
Channel 3	Secondary	/	/	Dry (sd)

Table 5: Definition of evaporative cooler categories based on channel type.

2.4. Description of evaporative cooler configurations

Evaporative coolers can be divided into three classes depending on how the evaporation process cools the primary air: direct evaporative coolers (DEC), indirect evaporative coolers (IEC), and two-stage evaporative coolers. The EC classes are discussed below, including a qualitative representation of air conditions in the evaporative exchanger using a psychrometric diagram. The latter intends to clarify the limiting conditions of each exchanger type by providing:

- The evolution of air conditions in an *actual* EC.
- The evolution of air conditions in an *ideal* EC, enhancing the physical limitations within the EC.
- A simplified energy balance (EB) by neglecting the energy term related to the water film.

The physical evolutions inside the evaporative coolers have been generated using numerical models developed by the authors, which will be the subject of a future paper.

2.4.1. Direct evaporative cooler (DEC)

A direct evaporative cooler consists only of primary wet channels, and its limiting temperature is the wet bulb temperature of the incoming air (Figure 2). Water and air enter the same channel, and cooling occurs through water evaporation. The wet bulb temperature is, by definition, the minimum temperature that air can reach when adiabatically cooled by water evaporation [52]. Consequently, in the ideal case, the air is humidified until saturation, and the lowest temperature that can be reached through direct humidification is the wet bulb temperature of the inlet air [53].

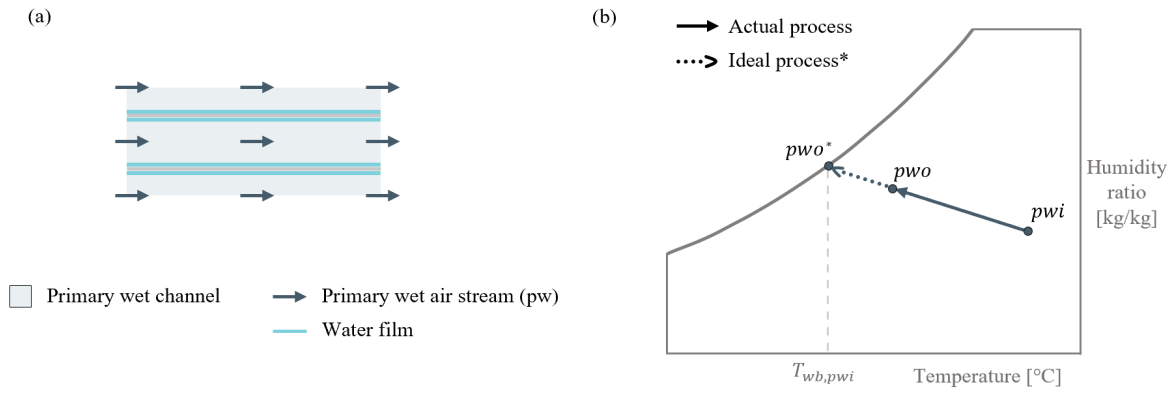

Figure 2: **DEC** (a) Stacked primary wet channels. (b) Psychrometric diagram showing the evolution of air conditions during an adiabatic humidification, ideally until the wet bulb temperature.

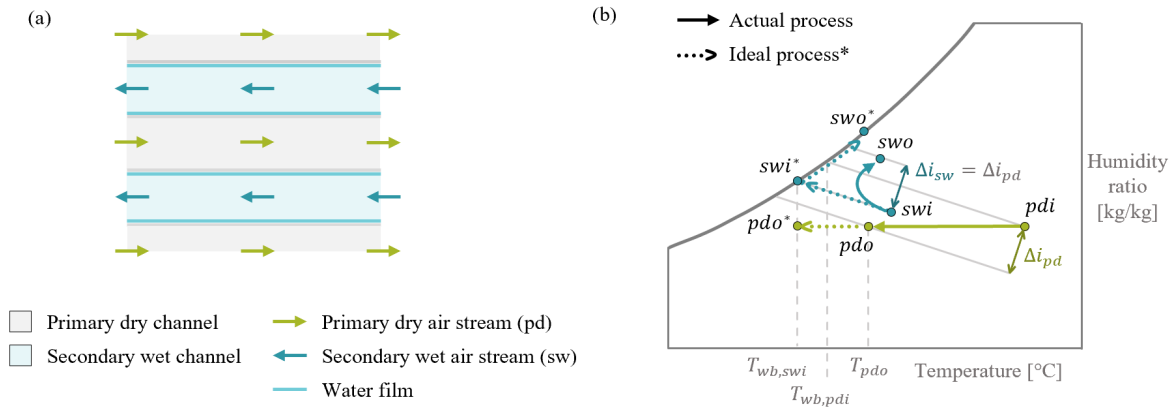

Figure 3: **IEC** (a) Alternation of primary dry channels and secondary wet channels. (b) Psychrometric diagram showing the evolution of air conditions with balanced airflow rates. The primary air is cooled sensibly, ideally until the secondary air inlet wet bulb temperature.

2.4.2. Indirect evaporative cooler (IEC)

An indirect evaporative cooler is composed of alternate layers of primary dry channels and secondary wet channels (Figure 3a). The inlet conditions of the secondary channel influence the lowest outlet temperature of the primary air. The evaporation process occurs in the secondary channel, in which the air experiences a cooling effect due to latent heat transfer from water evaporation and a sensible heating due to heat transfer with the primary dry channel. In the primary channel, the air is cooled without being humidified (Figure 3b) [49]. In the ideal process, the secondary air is humidified until saturation (swi^*) when entering the wet channel. The minimum temperature the primary air can achieve is thus the wet bulb temperature of the secondary air ($T_{wb,swi}$).

The advantage of IEC over DEC in building air conditioning is twofold. First, since primary air is sensibly cooled, it avoids humidification of the building. Second, the outlet temperature of the primary air can be lower than the inlet wet bulb temperature if the secondary air source of the IEC is chosen carefully. For example, in most building applications, the primary air source is the outdoor air, while the secondary air source is the indoor air extracted from the building. In very hot and humid climates, the indoor environment can be maintained at temperature and humidity levels such that the resulting primary outlet temperature is lower than its wet bulb temperature, or even its dew point temperature [54].

In the literature, configuration improvements have been proposed to decrease the minimum theoretical temperature of the IEC, which is the wet bulb temperature of the secondary air. The three most common configuration improvements are the partial regeneration of primary air, the addition of a secondary dry channel, and the perforation of the wall between dry and wet sides. Each technique aims to target the dew point temperature as the limit temperature. They are detailed below, and a qualitative representation of the evolution of air conditions inside the evaporative exchangers is given in a psychrometric chart.

Dew point indirect evaporative cooler (D-IEC)

In a dew point indirect evaporative cooler, part of the primary air is regenerated and used as secondary air in the wet channels, decreasing the minimum temperature to the dew point temperature of the primary air (Figure 4). This configuration was first referred to as *closed-loop* in the literature, as part of the primary air circulates in a closed-loop in the exchanger [44]. Lately, it has mainly been referred to as *regenerative* [30] or *dew point* [6] IEC.

Since part of the primary air is used as the secondary air source, a trade-off has to be found between the outlet air temperature and the produced cooled airflow rate. The higher the regeneration rate, the lower the primary air outlet temperature, but the lower the useful airflow rate. In the literature, it is common practice to consider a regeneration rate, or secondary-to-primary airflow rate ratio (SPR), of 0.3-0.4 to maximise the cooling capacity of the D-IEC

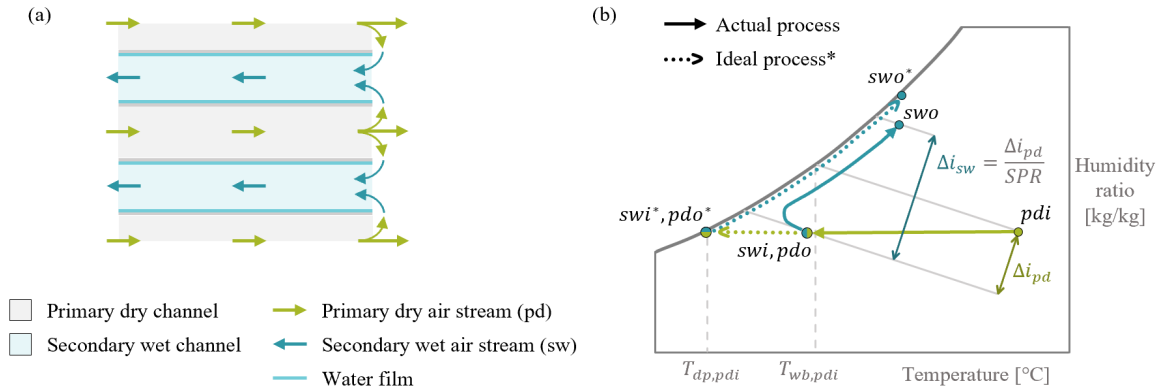

Figure 4: **D-IEC** (a) Alternation of primary dry channels and secondary wet channels. Part of the outlet primary air is recirculated in the secondary channels. (b) Psychrometric diagram showing the evolution of air conditions for an SPR of 0.5. The primary air is cooled sensibly, ideally until its dew point temperature.

[35, 36, 55].

Using a D-IEC instead of an IEC depends on the evaporative cooler integration into the building. A D-IEC requires only one airflow inlet, which can be more suitable for decentralised air conditioning.

Maisotsenko indirect evaporative cooler (M-IEC)

The Maisotsenko indirect evaporative cooler (also referred to as the *Maisotsenko cycle* [10]) is a sub-category of the indirect evaporative coolers that allows reducing their limit temperature by allocating one additional channel to the secondary side. This configuration was introduced by Professor Maisotsenko in the former USSR patents (SU No 979796) [9, 56]. This type of IEC is made of an alternation of three layers: primary dry channel, secondary wet channel, and secondary dry channel (Figure 5a). The secondary air is first sensibly cooled in a dry channel, before being used as secondary fluid in the wet channel. In the wet channel, the air experiences a cooling effect through the evaporation of water and a sensible heating due to heat transfer with both the primary and secondary dry channels (Figure 5b). In the ideal case, the secondary dry air can be cooled to its dew point temperature, which is consequently the theoretical lowest temperature the primary air can reach. As shown in Figure 5b, the primary air is cooled from T_{pdi} to T_{pdo^*}, the secondary dry air dew point temperature $T_{dp,sdi}$.

Using an M-IEC instead of an IEC depends on secondary air source conditions, application, and available space. Secondary air conditions can be such that it is possible to decrease the temperature of the primary air below its dew point temperature, inducing condensation within the primary channel, as shown in Figure 5b [54, 57]. However, compared to standard IEC, M-IECs are usually less compact because they require two secondary channels for one primary channel. M-IECs are generally used in applications in which the primary fluid to be cooled is not necessarily humid air, while benefiting from the cooling effect of water evaporation. The M-IEC can, for example, be integrated into power cycles to improve performance [56, 58].

Perforated D-IEC and M-IEC

The D-IEC and M-IEC configurations can be improved by perforating the wall between the dry and wet sides to divert the primary air gradually into the wet channel (Figure 6a). The perforations have contradictory effects on the thermal performance. On the one hand, mixing wet air with dry air decreases the relative humidity of the secondary airflow, initiating a new evaporation cycle (Figure 6b). On the other hand, the SPR is lower than its nominal value in most of the channel length (Figure 6a), reducing performance. Güzelel et al. [35] showed that performance improvement due to perforations is strictly related to the global SPR of the exchanger, *i.e.*, there exists an SPR above which the perforated configuration performs better than the reference one.

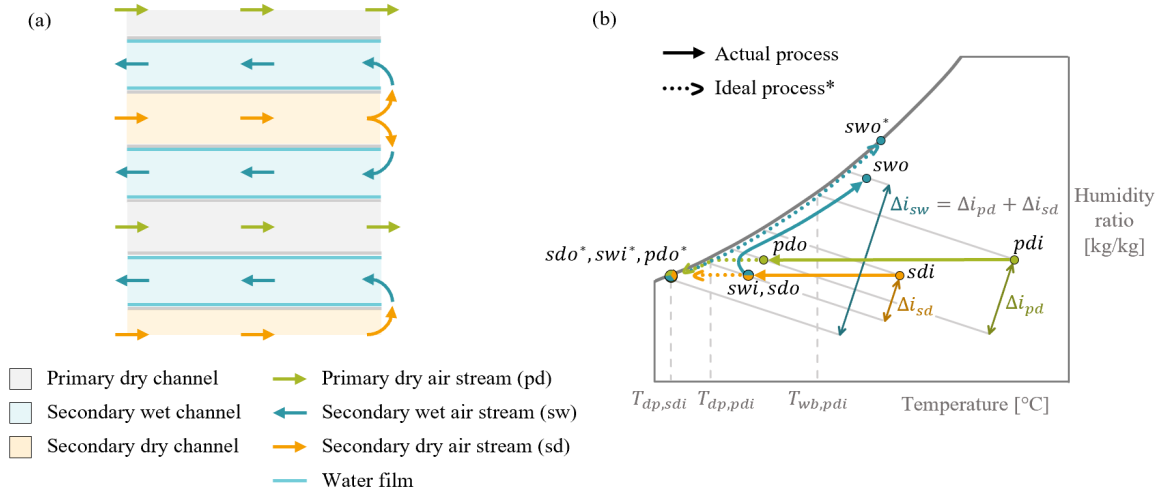

Figure 5: **M-IEC** (a) Alternation of primary dry channels, secondary wet channels, and secondary dry channels. (b) Psychrometric diagram showing the evolution of air conditions. The primary air is cooled sensibly, ideally until the secondary air dew point temperature. Under specific operating conditions, condensation can appear in the primary channel.

Regarding hydraulic performance, perforations significantly decrease the pressure drop in the EC because less air flows into the channels. Although perforations can disrupt the flow, the latter remains mostly laminar [35]. Figure 6 shows a schematic representation of a perforated D-IEC, and the evolution of the air conditions in a psychrometric diagram for one perforation only to facilitate reading of the graph.

2.4.3. Two-stage IEC

A two-stage EC integrates two EC variants in one single device. The most common two-stage EC configurations include combinations of IEC, D-IEC and DEC in series [39]. Anisimov et al. [59, 60] proposed a novel IEC configuration, combining a standard IEC module and a D-IEC module. The standard IEC module acts as a pre-cooler for the D-IEC to get closer to the dew point temperature at the outlet of the primary channel. Such a configuration is referred to as *combined*, or *multi-stage* IEC [51]. A typical example of a two-stage IEC is shown in Figure 7, along with the evolution of air conditions in the psychrometric diagram. The minimum achievable temperature under ideal operation is the dew point temperature of primary air.

2.5. Performance evaluation

The performance of evaporative coolers can be assessed using various indicators depending on one's interest in the cooling system or the evaporative cooling device itself. System-oriented indicators generally include cooling capacity, water consumption, and coefficient of performance (COP) [35] while the thermal performance of evaporative cooling devices is generally assessed with the wet bulb and the dew point effectivenesses [37]. Since the thermal performance of devices depends on outdoor conditions, it has been shown that the feasibility of systems including evaporative cooling should be studied before evaluating their COP [61].

In this paper, performance assessment is device-oriented and the chosen indicators are the wet bulb and the dew point effectivenesses. Those effectivenesses can be used to effectively compare the performance of several evaporative cooler configurations or two evaporative coolers with a similar configuration under similar operating conditions on the primary side [37]. They provide information on the *sensible* heat transfer occurring in the evaporative cooler by comparing the actual temperature decrease to a reference one. Both effectivenesses are defined below.

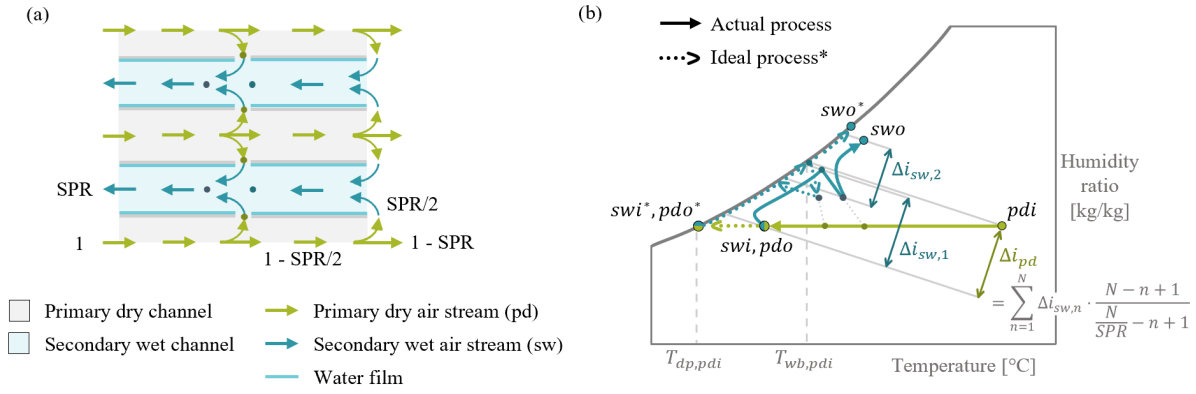

Figure 6: **Perforated D-IEC** (a) Alternation of primary dry channels and secondary wet channels with the recirculation of part of the primary air in the secondary channels at the location of the perforation and the end of the channel. (b) Psychrometric diagram showing the evolution of air conditions for an SPR of 0.5. The primary air is cooled sensibly, ideally until its dew point temperature.

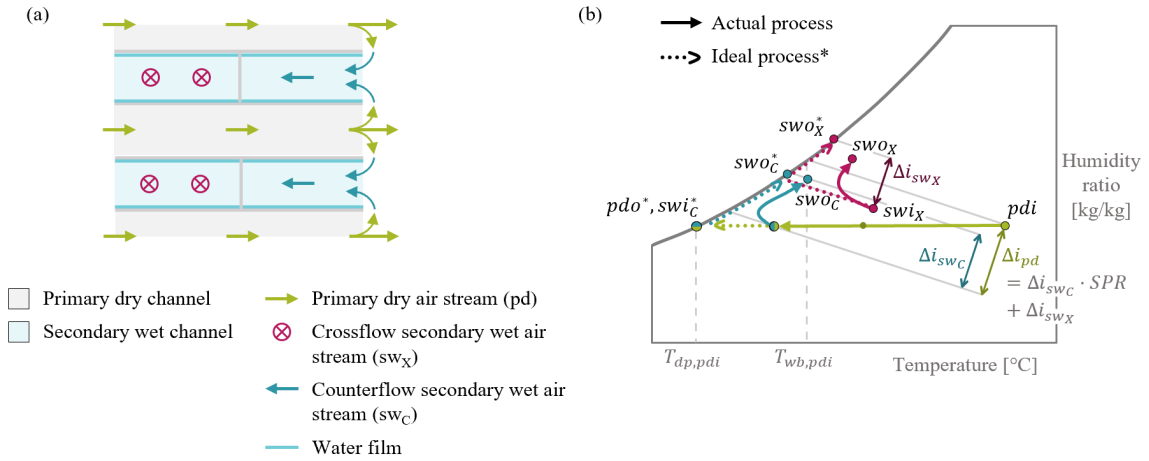

Figure 7: **Two-stage IEC** (a) Alternation between primary dry channels and secondary wet channels. Secondary wet channels are divided into a crossflow section and a counterflow section with regeneration of the primary air. (b) Psychrometric diagram showing the evolution of air conditions with an SPR of 0.5 in the counterflow part. The primary air is cooled sensibly, ideally until its dew point temperature.

2.5.1. Wet bulb effectiveness

The wet bulb effectiveness compares the actual evolution with an adiabatic humidification, for which the minimum achievable temperature is the *wet bulb temperature*:

$$\varepsilon_{wb} = \frac{T_{p,i} - T_{p,o}}{T_{p,i} - T_{wb,p,i}} \tag{1}$$

This indicator is best suited for direct evaporative coolers, to compare their performance with an ideal humidification. However, it is also often computed for IECs and M-IECs to determine if they are more efficient than direct humidification of primary air.

2.5.2. Dew point effectiveness

The dew point effectiveness compares the actual evolution with sensible cooling until saturation, which would ideally occur in indirect evaporative coolers. In this case, the primary air dew point temperature is used as a reference for the minimum achievable temperature:

$$\varepsilon_{dp} = \frac{T_{p,i} - T_{p,o}}{T_{p,i} - T_{dp,p,i}} \tag{2}$$

The main advantage of the dew point effectiveness is that it allows an immediate comparison of indirect evaporative cooler configurations based only on primary air conditions by illustrating the proximity to saturation.

2.5.3. Actual effectiveness

The dew point and wet bulb effectivenesses do not necessarily reflect the real performance of IECs because they only consider the operating conditions on the primary side. For some ECs, they cannot be used to evaluate the closeness of the EC to an ideal one. For example, standard IECs generally show less good performance than D-IEC [62] because the minimum reachable temperature in an IEC is the wet bulb temperature of the secondary air, which is often higher than the dew point of the primary air. Conversely, the efficiency of M-IEC can be overestimated by using the dew point efficiency since their minimum theoretical temperature is the dew point temperature of the secondary air. Their performance can be enhanced by selecting a secondary fluid that is less humid than the primary fluid, by using the return air in a building, for example.

To study the real performance of evaporative coolers, a general form of the effectiveness can be defined. Equation 3 can be adapted depending on the evaporative cooler configuration by using the corresponding minimum temperature.

$$\varepsilon = \frac{T_{p,i} - T_{p,o}}{T_{p,i} - T_{min}} \tag{3}$$

The values of T_{min} can be found in Table 6 for each evaporative cooler configuration. The table also provides a comparison of the advantages and drawbacks of each configuration and their typical applications.

3. Methodology

This section introduces the methodology applied in this work to obtain standardised datasets for each evaporative cooler configuration. Section 3.1 presents the variables reported in the datasets and Section 3.2 introduces the selection procedure of the reference papers and the data standardisation method.

3.1. Identification of evaporative cooler characteristics

This section presents the variables reported in the datasets. Section 3.1.1 recalls the physical equations of evaporative coolers to identify the parameters required to develop a numerical model. Section 3.1.2 identifies the geometrical parameters of a standard evaporative cooler. Section 3.1.3 details the calculation method applied to obtain the heat transfer coefficient inside the evaporative coolers, when not discussed in the investigated paper. Section 3.1.4 defines the two identified water injection strategies, which can impact the operation and modelling of evaporative coolers.

Config.	T_{min}	Advantages	Drawbacks	Application	Ref.
DEC	$T_{wb,pwi}$	Simple design, good performance, low energy consumption.	Humidification of primary air.	Building with limited indoor space and mechanical supply only, in dry climate zones.	[39, 40]
IEC	$T_{wb,swi}$	Simple design, no humidification of primary air, low water consumption.	Outlet conditions depend on the inlet conditions on the secondary side and limited cooling effectiveness.	Building with both mechanical supply and extraction and limited indoor space. Enhanced cold recovery module in HVAC systems.	[35, 61, 63]
D-IEC	$T_{dp,pdi}$	Decreased outlet temperature.	Trade-off between outlet temperature and useful airflow rate.	Building with limited indoor space and mechanical supply only. Pre-cooling module in complex HVAC systems.	[6, 64, 65]
Perforated D-IEC	$T_{dp,pdi}$	Reduced pressure losses.	Reduced thermal performance at low SPR compared to the non-perforated configuration.	Same applications as D-IEC.	[10, 35]
M-IEC	$T_{dp,sdi}$	Reduced dependency on secondary air conditions, possibility to use a different fluid than humid air as primary fluid.	Higher pressure losses, less compactness.	Building with dedicated space and strict requirements on supply temperature. Industrial processes (power cycles).	[35, 56–58]
Two-stage IEC	$T_{dp,pdi}$	Decreased outlet temperature. Combinations inducing a DEC limit the increased humidity content of primary air.	For combination of cross/counterflow, use of three airflows, inducing the need for an additional fan.	Building with dedicated space and strict requirements on supply temperature.	[59, 60, 66]

Table 6: Comparison of the existing evaporative cooler configurations. The perforated M-IEC is not reported in the Table as it combines the advantages and drawbacks of the M-IEC and the perforated D-IEC.

3.1.1. Physical equations of evaporative coolers

The purpose of this section is to present a set of parameter combinations that can be used to validate an evaporative cooler model. The physical equations resulting from a mass and energy balance over a differential element of an evaporative cooler lay the basis for the establishment of the necessary parameters to develop a numerical model.

The physical equations of evaporative coolers are given for an IEC, but they can easily be derived for the direct configuration. The following assumptions are often considered in the literature [36, 67–69]:

(a) steady-state and fully developed flow;
(b) zero wall, air thermal, and moisture diffusivity in the flow direction;
(c) no heat transfer to the surroundings;
(d) constant specific heat;
(e) constant heat and mass transfer coefficients and Lewis factor along the heat exchanger surface;
(f) negligible thermal conduction resistances of wall and water film;
(g) air-water interface temperature equal to the bulk water temperature;
(h) air saturation at the air-water interface;
(i) water film spread uniformly on the wetted surface.

The physical equations of indirect evaporative coolers can be derived from energy and mass conservation principles for a differential element, as represented in Figure 8.

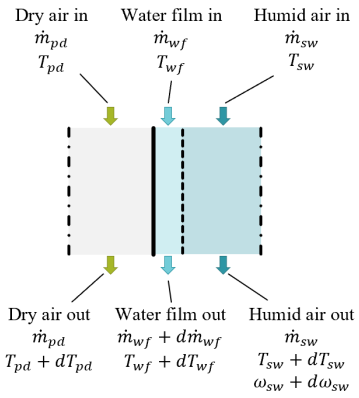

Figure 8: Representation of a differential element for a parallel flow indirect evaporative cooler.

Energy balance equation for cooling air (sw):

$$\dot{m}_{sw}\mathrm{d}i_{sw} = [h_{T,sw}(T_{wf} - T_{sw}) + h_D(\omega_{wf} - \omega_{sw})]A_a\mathrm{d}x_{sw} \tag{4}$$

Mass balance equation for cooling air and water (wf):

$$\dot{m}_{sw}\mathrm{d}\omega_{sw} = h_D(\omega_{wf} - \omega_{sw})A_a\mathrm{d}x_{sw} \tag{5}$$

$$\mathrm{d}\dot{m}_{wf} = -\dot{m}_{sw}\mathrm{d}\omega_{sw} \tag{6}$$

Energy balance equation for cooled fluid (pd):

$$\dot{m}_{pd}c_{p,pd}\mathrm{d}T_{pd} = h_{T,pd}(T_{wf} - T_{pd})A_a\mathrm{d}x_{pd} \tag{7}$$

Energy balance equation for the differential element:

$$\dot{m}_{pd}c_{p,pd}\mathrm{d}T_{pd} + c_{p,wf}T_{wf}\mathrm{d}\dot{m}_{wf} + \dot{m}_{wf}c_{p,wf}\mathrm{d}T_{wf} + \dot{m}_{sw}\mathrm{d}i_{sw} = 0 \tag{8}$$

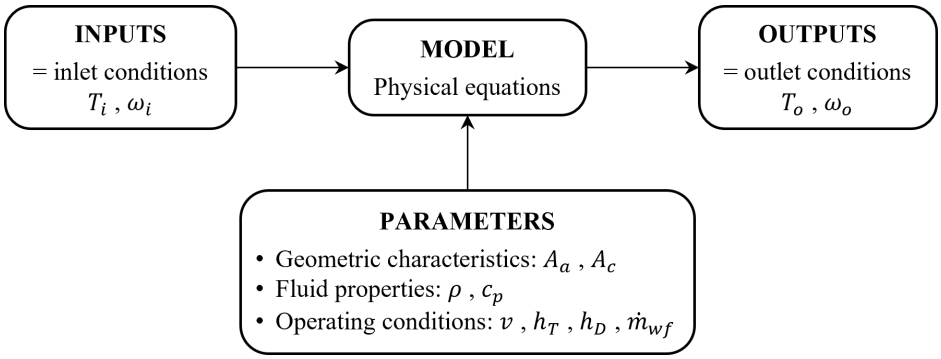

Figure 9: Identified model parameters from the development of the physical equations.

All the parameters identified in Equations 4-8 are summarised in Figure 9. For all datasets, the parameters have been identified based on the values presented in the reference papers or computed using well-known correlations, depending on data availability.

- The inlet and outlet conditions are generally given directly in the reference paper, either in the form of tables or in graphs. In some cases, the outlet conditions can also be derived from the energy balance computation.
- The geometric characteristics are defined in Section 3.1.2 for a generic evaporative cooler.
- The fluid properties should be computed at the average temperature of each fluid stream and are assumed constant along the channel.
- The airflow velocities are directly given in the reference papers as part of the operating conditions.
- The water flow rate depends on the injection technique, as discussed in Section 3.1.4.
- The heat transfer coefficient can be computed using various correlations. The method presented in Section 3.1.3 was applied to cases in which no heat transfer correlation was presented in the reference paper.
- The mass transfer coefficient, it is often computed in the literature by considering a unitary Lewis number [70]:

$$Le = \frac{h_T}{h_D c_p} \tag{9}$$

3.1.2. Geometric characteristics

The geometric characteristics of the evaporative coolers are given for a corrugated plate heat exchanger to generalise the parameter calculation. The nomenclature related to the geometry of the exchanger is given in Figure 10. The transfer surface area and the cross-sectional area can be computed as:

$$A_a = 2 \cdot A_{wall} = 2 \cdot L \cdot W^* \tag{10}$$

$$A_c = h_{ch} \cdot W \tag{11}$$

The hydraulic diameter D_h of a heat exchanger with a low aspect ratio can be computed as:

$$D_h = \frac{4A_c}{P} = \frac{4h_{ch}W}{2(h_{ch} + W^*)} \simeq \frac{2h_{ch}}{WWR} \tag{12}$$

with WWR, the effective to actual width ratio:

$$WWR = \frac{W^*}{W} \tag{13}$$

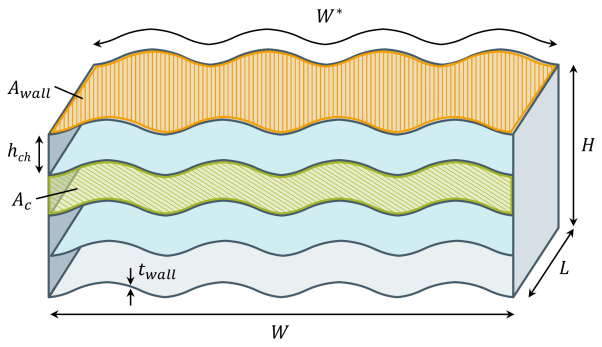

Figure 10: Simplified schematic of an IEC introducing the nomenclature related to the exchanger geometry.

3.1.3. Heat transfer coefficient

Various correlations exist to compute the Nusselt number or the heat transfer coefficient in a (corrugated) plate heat exchanger [30]. This section introduces the calculation method used to compute the heat transfer coefficients for papers that do not detail the specific correlations used in the frame of their study. The heat transfer coefficients have been computed for information purposes, and it cannot be ensured that the use of this value in a numerical model shall yield the same results as in the reference papers.

The heat transfer coefficient of air inside a channel depends mainly on the geometry of the channel and the properties of air. It is given by:

$$h_T = \frac{Nu \cdot k}{D_h} \tag{14}$$

The Nusselt number should be computed differently depending on the flow type and the heat exchanger geometry. In this section, the presented computation method of the Nusselt number is based on the book of reference on heat transfer written by Nellis and Klein [71]. For an internal airflow, the flow can be considered laminar if

$$Re = \frac{D_h \cdot v}{\nu} < 2300 \tag{15}$$

For a laminar developed flow in a rectangular duct with a low aspect ratio, the Nusselt number equals 7.54 for a constant wall temperature and 8.23 for a constant heat flux (Shah and London, 1978).

In case of a turbulent airflow, the Nusselt number is not affected by the duct shape or boundary conditions, but it is sensitive to the surface roughness. The Nusselt number for fully developed turbulent flow is provided by Gnielinski (1976):

$$Nu = \frac{f/8(Re - 1000)Pr}{1 + 12.7(Pr^{2/3} - 1)\sqrt{f/8}} \qquad \text{for} \quad 0.5 < Pr < 2000 \quad \text{and} \quad 2300 < Re < 5 \cdot 10^6 \tag{16}$$

where f is the fully developed friction factor, which can be obtained through the explicit correlation proposed by Zigrang and Sylvester (1982):

$$f = \left(-2 \cdot \log\left(\frac{2e}{7.54D_h} - \frac{5.02}{Re}\log\left(\frac{2e}{7.54D_h} + \frac{13}{Re}\right)\right)\right)^{-2} \tag{17}$$

The factor e/D_h represents the relative pipe roughness and has been arbitrarily set at 0.005, as it has a low influence on the friction factor value for low Reynolds numbers.

3.1.4. Water injection

The water injection strategy can impact the evaporative cooler operation and modelling. Sadighi Dizaji et al. [47, 72] defined two water injection processes: wet surface and sprayed water.

In the *wet surface* process, the water forms a uniform film of negligible thickness on the surface of the wet channel. In the first evaporative cooler models developed, the evaporating water film was assumed stationary and continuously replenished with water at the same temperature [73], which implies a low injected water flow rate compared to the airflow rate.

In the *sprayed water* process, water is sprayed inside the evaporative cooler, and the water flows along the wet channel, forming a separate fluid that exchanges with the air within the same channel. When the water is sprayed inside the heat exchanger, its mass flow rate cannot be neglected compared to the airflow rate. The water temperature is also important as it can exchange sensible heat with the air [67].

3.2. Database generation

Datasets were generated based on data from reference papers. This section details the selection procedure of the reference papers and the methodology applied to obtain standardised datasets.

3.2.1. Selection procedure

Datasets were selected to form a database for the validation of evaporative cooler models under various operating conditions. The conditions to consider a reference paper to be included in the database are the following:

- The paper should contain enough information to ensure reproducibility.
- The aggregation of datasets should span a large range of operating conditions.
- Datasets include both experimental and numerical data. Experimental datasets are used to validate the model against real data, while numerical datasets enable a comparative model validation.
- Two types of datasets are presented in this paper, depending on the validation process that can be applied. Validation can be performed based on the air conditions at the inlet and outlet of the exchanger or based on the evolution of the air conditions inside the exchanger.

3.2.2. Data standardisation and reproducibility

The datasets have been assembled by collecting data from reference papers, by filling an Excel template gathering the information and variables presented in Section 3.1. Data has been collected from the reference paper, and the nomenclature has been unified according to the nomenclature presented in this paper.

The useful data is presented in the form of a test matrix, including the testing conditions (exchanger geometry and heat transfer characteristics), inlet air and water conditions, and outlet air conditions. The standardisation of data involves normalising all the results for a single channel. The outlet air conditions could be found in three main forms:

- Data was given in the form of a Table in the reference paper, ensuring the largest confidence in the data.
- Data was given in the form of graphs. In this case, the values were extracted using *PlotDigitizer*, an online software that can extract data from images of graphs, plots, and charts. The digitisation process introduces a negligible source of error in the data, regarding the software accuracy.
- Data was not directly given in the paper. In this case, the outlet air conditions had to be computed based on performance indicator definitions or based on energy conservation equations.

Information		Kovačević and Sourbron [45]	Wu et al. [79]	Nada et al. [80, 81]
		Description		
Method		Exp & num	Exp & num	Exp
Configuration		XF	XF	XF
Water injection		Wet surface	Wet surface	Sprayed-water
Dataset size		27	82	85
		Parameters		
L	m	0.09	0.1-0.4	0.035-0.14
h_{ch}	mm	4.16	6	7
W	m	-	0.3	0.47
WWR		1.141	1	1.1
nb_{ch}		-	-	53
Re		420-1350$^{(d)}$	730-2915$^{(d)}$	700-2300$^{(d)}$
Nu		7.54	7.54-9.73$^{(d)}$	7.54$^{(d)}$
h_T	W/m².K	26.1-28.2$^{(d)}$	16.5-21.7$^{(d)}$	15.8-16.6$^{(d)}$
T_{pwi}	°C	21-36	27.2-37.1	30-50
ω_{pwi}	g/kg	2.6-23.6	6-17.6	6-11$^{(c)}$
v_{pwi}	m/s	1-3	1-4	1-3
T_{wfi}	°C	-	-	25-40
$\dot{V}_{wf}$	L/h	-	-	3.2-11.3
T_{pwo}	°C	8-31.1	22.4-31.2	21.1-39.9$^{(a)}$
ω_{pwo}	g/kg	6.8-28.3$^{(c)}$	10.3-20.2$^{(c)}$	6-19$^{(a)}$
ε_{wb}		0.85-0.99$^{(d)}$	0.38-0.94$^{(d)}$	0-0.83$^{(a)}$

Table 7: Summary of selected datasets for the validation of DEC models. Unless otherwise specified, all data are directly provided in the reference paper. $^{(a)}$*Data extracted from graph.* $^{(b)}$*Data computed with equations provided in the reference paper.* $^{(c)}$*Data obtained through EB.* $^{(d)}$*Data computed with equations presented in this paper.*

4. Presentation of selected datasets for model validation

As detailed in Section 3.2, the selected datasets offer the possibility to validate an evaporative cooler model in various operating ranges. For each evaporative cooler configuration, several datasets were selected. This section briefly describes each dataset and provides a recapitulative table of the dataset characteristics for each EC configuration. All datasets can be found in an open-source database.

4.1. Direct evaporative cooler (DEC)

The most studied DEC configuration is crossflow [40]. The air flows horizontally through a pad coated with a water-absorbing material, and cooling water is sprayed on the top of the pad and flows down the cooler core through gravitational effect [11]. Many models have been developed and validated in the literature [74–78], but there are only a few studies that provide sufficient information to be reproduced. Table 7 presents a summary of the key characteristics of the selected studies.

Wu et al. [79] experimentally studied a crossflow DEC. The DEC matrix is made of a GLASdek pad material with a cross-fluted, unequal angle pad design to induce turbulent mixing of air and water for optimum heat and moisture transfer. They first compared their simulation results with experimental data, showing a good agreement between

both. Then, they studied the impact of inlet temperature and humidity, air velocity, and pad length on the DEC efficiency. They found that the inlet air conditions have a low impact on the wet bulb efficiency, while the length of the evaporative cooler highly impacts its performance.

Kovačević and Sourbron [45] experimentally tested a finned DEC with water sprayed perpendicularly to the main airflow direction. The aluminium fins increase the effective contact area between air and water, hence increasing the DEC effectiveness. Experimental results used for model validation are presented, with a good agreement between predicted and measured data. The numerical model was then used to investigate the impact of the inlet conditions on the DEC performance. They found that air velocity determines the pad effectiveness, with lower velocities giving higher effectiveness, and vice versa. The relative humidity drastically influences the water evaporation rate while not impacting effectiveness. An increasing inlet air temperature slightly increases effectiveness and water consumption.

Nada et al. [80, 81] tested a new evaporative cooling pad material made of 0.7 mm thick cellulose corrugated sheets assembled in a "bee-hive" structure. The thermal and hydraulic performance of the DEC was studied for a wide range of operating conditions and geometric parameters. The cooling pad length was varied by arranging 1 to 4 pads in series. They also studied the impact of varying the air velocity, the inlet air temperature, and the humidifier water temperature and flow rate. They observed that the water temperature has a significant impact on DEC performance.

4.2. Standard indirect evaporative cooler (IEC)

The standard IEC is the simplest configuration of IEC. In the literature, it is mainly studied with a crossflow arrangement [34]. The studies that have been selected for model validation of the IEC are described below. Their main characteristics are summarised in Table 8.

4.2.1. Experimental studies

De Antonellis et al. [68] experimentally studied a crossflow IEC, consisting of a commercial 118-channel plate heat exchanger with water spray nozzles installed at the inlet of the secondary channels. They investigated the effect of the secondary air inlet conditions and sprayed water flow rate on the performance of the heat exchanger. The main interest of this data set lies in the measurement of the air conditions at the outlet of the secondary channel, which implies the possibility of performing a model validation on the secondary side as well.

De Antonellis et al. [82] also investigated the effect of water nozzles and airflow arrangement on the IEC described above by testing 6 different orientations. In this study, outlet conditions have been measured for the primary air temperature only. It is also interesting to note that in their paper, the authors do not propose a way to adapt the numerical model parameters to account for the exchanger orientation.

4.2.2. Numerical studies

Most IEC models are based on the analytical equations developed by Ren and Yang [67] for parallel and counterflow configurations. They proposed a set of differential equations for the primary air and water film temperatures and for the secondary air temperature and humidity ratio, using dimensionless coefficients. They provided the results of the analytical model resolution and of their numerical model for various coefficient combinations. The use of this dataset is thus relevant only if the formalism of the numerical model is similar to the one proposed by Ren and Yang.

Shi et al. [83] developed a numerical model, which was validated based on the work of De Antonellis et al. [82]. They used this model to investigate the effect of two water spraying techniques on the IEC performance. Contrary to De Antonellis et al., who focused on the impact of secondary air conditions on the primary air outlet temperature, Shi et al. considered variable conditions for the primary air inlet temperature.

4.3. Dew point indirect evaporative cooler (D-IEC)

The D-IEC is the most studied configuration in the literature, most often in counterflow configuration [34]. The studies that have been selected for model validation of the D-IEC are described below. Their main characteristics are summarised in Table 9.

Information		Ren & Yang [67]	De Antonellis et al. [68]	De Antonellis et al. [82]	Shi et al. [83]
			Description		
Method		Num	Exp	Exp	Num
Configuration		CF	XF	XF	CF
Water injection		Both	Sprayed-water	Sprayed-water	Wet surface
Dataset size		16	59	120	68
			Parameters		
L	m	-	0.47	0.47	0.4
h_{ch}	mm	-	3	3	4-5
W	m	-	0.47	0.47	-
WWR		1	1	1	1
nb_{ch}		-	118	118	-
Re		-	756-1490$^{(d)}$	1450-1480$^{(d)}$	750-2180$^{(d)}$
Nu		-	7.54$^{(d)}$	7.54$^{(d)}$	7.54$^{(d)}$
$h_{T,pd}$	W/m².K	-	32.0-59.9$^{(b)}$	31.1-31.4$^{(d)}$	19.7-25.3$^{(d)}$
$h_{T,sw}$	W/m².K	-	32.0-88.7$^{(b)}$	31.1-31.4$^{(d)}$	19.7-25.3$^{(d)}$
T_{pdi}	°C	21-36	30, 35	35	24-36
ω_{pdi}	g/kg	-	10	10	7-15
v_{pdi}	m/s	-	1.9-3.7	3.7	1.5-3.5
SPR		0.08-1.33	1-1.54	1-1.54	0.33-1.33
T_{swi}	°C	21-50	30-40	30-36.8	25
ω_{swi}	g/kg	-	11-13	11-13	12
T_{wfi}	°C	-	-	-	-
$\dot{V}_{wf}$	L/h	-	0.5-1	0.5-1.1	-
T_{pdo}	°C	18.5-35	23.2-29.4$^{(a)}$	21.9-28.8$^{(d)}$	21.1-31$^{(d)}$
T_{swo}	°C	19-32	24.4-27.9$^{(a)}$	-	-
ω_{swo}	g/kg	12-40	15-19$^{(a)}$	-	-
ε_{wb}		-	0.59-0.91$^{(d)}$	0.45-0.94$^{(a)}$	0.24-0.66$^{(a)}$
ε_{dp}		-	0.39-0.6$^{(d)}$	0.30-0.62$^{(d)}$	0.14-0.44$^{(d)}$

Table 8: Summary of selected datasets for the validation of IEC models. Unless otherwise specified, all data are directly provided in the reference paper. $^{(a)}$*Data extracted from graph.* $^{(b)}$*Data computed with equations provided in the reference paper.* $^{(c)}$*Data obtained through EB.* $^{(d)}$*Data computed with equations presented in this paper.*

Information		Riangvilaikul & Kumar [84]	Lin et al. [85]	Liu et al. [86]	Pakari & Ghani [87]	Lin et al. [55]	Kashyap et al. [69]
				Description			
Method		Exp	Exp	Exp	Exp & num	Exp	Num
Configuration		CF	CF	CF	CF	CF	CF/XF
Water injection		Wet surface	Wet surface	Sprayed-water	Wet surface	Wet surface	Sprayed-water
Dataset size		30	2	17	105	17	368
				Parameters			
L	m	1.2	0.8	1.05	0.5-1	0.6	0.5
h_{ch}	mm	5	4	4.3	2-5	3	3-7
W	m	0.08	0.18	0.716	0.3	0.15	0.5
WWR		1		1.1	1	1	1
nb_{ch}		9	4	234	100	20	140
Re		883-3643$^{(d)}$	1032, 983$^{(d)}$	830-1210$^{(d)}$	127-678$^{(d)}$	418-764$^{(d)}$	615-1850$^{(d)}$
Nu		8.23-17.7	8.23	8.23	2.81	7.54$^{(d)}$	15.3 -25.0$^{(b)}$
$h_{T,pd}$	W/m².K	21.3-47.3$^{(d)}$	29.7, 29.9$^{(a)}$	27.3-28.1$^{(d)}$	7.5-18.9$^{(d)}$	32.9-33.5$^{(d)}$	39.5-92.4$^{(b)}$
$h_{T,sw}$	W/m².K	21.3-22.4$^{(d)}$	29.4, 29.2$^{(a)}$	27.3-28.1$^{(d)}$	20.1-50.7$^{(d)}$	32.9-33.5$^{(d)}$	23.3-54.6$^{(b)}$
T_{pdi}	°C	25-45	32.6, 38.2	25-39	25-45	30-40	35
ω_{pdi}	g/kg	7-26	14, 10.2	6-15	3-19	11	8-25
v_{pdi}	m/s	1.45-6	2.1, 2	1.6-2.5	0.5-1.5	1.1-2	1-3.3
SPR		0.33	0.32, 0.31	0.36-0.54	0.15-0.5	0.22-0.9	0.3-0.7
T_{wfi}	°C	-	20, 17	20-27	-	-	17-27
$\dot{V}_w$	L/h	0.012	-	3-8	-	-	0-60
T_{pdo}	°C	15.6-32.1$^{(a)}$	21.9, 20.0	17.2-25.4	13.6-32.6	15.9-23.4$^{(a)}$	17.9-30.9$^{(d)}$
T_{swo}	°C	-	29.5, 31.6	-	-	23.6-35.7$^{(a)}$	-
ω_{swo}	g/kg	-	23, 24$^{(c)}$	-	-	16-28$^{(c)}$	-
ε_{wb}		0.72-1.14$^{(d)}$	1.13, 1.13	0.75-1.08	0.45-1.23	0.88-1.45$^{(d)}$	0.5-1.3$^{(d)}$
ε_{dp}		0.48-0.84$^{(a)}$	0.80, 0.75	0.43-0.74	0.29-0.89$^{(d)}$	0.59-0.98$^{(d)}$	0.3-0.9$^{(a)}$

Table 9: Summary of selected datasets for the validation of D-IEC models. Unless otherwise specified, all data are directly provided in the reference paper. $^{(a)}$*Data extracted from graph.* $^{(b)}$*Data computed with equations provided in the reference paper.* $^{(c)}$*Data obtained through EB.* $^{(d)}$*Data computed with equations presented in this paper.*

4.3.1. Experimental studies

Riangvilaikul & Kumar [84] produced one of the most cited papers on the experimental studies of D-IEC. Their experimental results are often used in the literature for model validation. The studied D-IEC has a counterflow configuration and is made of vertical thin-film cotton sheets coated with polyurethane material. The water is sprayed on top of the wet channel, and the water distribution on the wet channel surface is ensured through gravitational effect. The advantage of the dataset provided by Riangvilaikul and Kumar is twofold. First, the experiments were performed to independently test the impact of primary inlet air conditions and velocity on the primary outlet temperature. Second, the tested inlet air conditions cover a large area of the psychrometric diagram.

Lin et al. [85] designed a horizontal 4-channel counterflow D-IEC with an impervious polymer sheet to separate the dry and wet channels. A piece of natural-fiber cellulose was pasted on the wet channel side to absorb and retain water. They investigated the temperature and humidity distributions of the primary air, secondary air, and water film by placing 8 RTD temperature sensor probes along the channels in each of the three flows. The evolution of the temperature profiles inside the exchanger is provided for two sets of inlet conditions.

Lin et al. [55] also engineered a horizontal 20-channel counterflow D-IEC with a Polyethylene Terephthalate (PET) sheet between dry and wet channels. A thin sheet of absorbent material covers the wet channel surface, allowing water to circulate through capillary action. They evaluated the impact of the primary air temperature and velocity at the heat exchanger inlet and the recirculation ratio on the primary and secondary air outlet temperature. The outlet specific humidity of the secondary air was not provided in the reference papers, but it was computed by performing an energy balance on the evaporative cooler to be included in the datasets.

Liu et al. [86] proposed an experimental setup of a D-IEC similar to a cooling tower in its construction to investigate the effect of water temperature and water flow rate on the primary air outlet temperature. The core of the exchanger is made of 235 vertical aluminium plates, coated with a high-wettability porous fibre on the wet channel side. The water is distributed in the wet channels by spraying. Liu et al. focused on the impact of the sprayed water characteristics on the primary air outlet temperature. They found that the temperature and water flow rate should be adjusted to optimise the performance of the D-IEC for large water-to-air flow rate ratios.

4.3.2. Numerical studies

Parkari and Ghani [87] numerically tested 90 combinations of geometrical parameters and operating conditions to evaluate the performance of D-IEC. To validate their model, they experimentally tested a vertical 100-channel D-IEC with dry channels made of corrugated plastic sheets stacked next to each other, and wicking paper pasted on the wet channels to enhance their wettability. The cooling system was tested by varying the primary air extraction ratio and the inlet air conditions (temperature, relative humidity, and velocity).

Kashyap et al. [69] developed a numerical D-IEC model that can be applied to various flow arrangements. Their numerical model was validated using the experimental results of Riangvilaikul and Kumar [84]. Then they compared 8 D-IEC configurations: 4 parallel/counterflow and 4 crossflow configurations. They compared their performance under varying operating conditions and geometric parameters. They also studied the effect of water temperature and flow rate, extraction ratio of primary air, gap size between channels, primary air velocity, and inlet wet bulb temperature.

4.4. Variations of the D-IEC configuration

The most common variations of the D-IEC are often studied together in the literature to compare their performance; hence, they have been gathered in a single section. The studies selected for model validation of the D-IEC and M-IEC variations are described below. As most studies in the literature regarding D-IEC variations, the datasets have all been generated numerically. Their main characteristics are summarised in Table 10.

Cui et al. [57] developed a CFD model for an M-IEC. Their model was validated for the D-IEC configuration only, using two data sources from the literature. First, the temperature profile of the air inside the primary channel was validated based on experimental results from Hsu et al. [44]. The model was further validated by comparing the

Information		Cui et al. [57]	Anisimov et al. [36]	Güzelel et al. [35]
		Description		
HEX type:				
IEC				✓
D-IEC			✓	✓
Perforated D-IEC			✓	✓
M-IEC		✓	✓	✓
Perforated M-IEC			✓	✓
Method		Num	Num	Num
Configuration		CF	CF/XF	CF
Water injection		Wet surface	Wet surface	Wet surface
Dataset size		39	103	108
		Parameters		
L	m	0.3-2	0.5	1
h_{ch}	mm	6-10	4	2.5
W	m	1	0.5	-
WWR		1	1	1
nb_{ch}		-	125	-
nb_{perf}		-	4	4
Re		720-3100$^{(d)}$	1007-3002$^{(d)}$	306-1520$^{(d)}$
Nu		11.5-25.8$^{(b)}$	4.12-14.4	7.54$^{(d)}$
$h_{T,pd}$	W/m².K	15.2-36.8$^{(b)}$	13.3-47.5$^{(d)}$	39.4-40.9$^{(d)}$
$h_{T,sw}$	W/m².K	40.7-61.3$^{(b)}$	13.3-62.9$^{(d)}$	39.4-40.9$^{(d)}$
T_{pdi}	°C	25-40	25-45	25-45
ω_{pdi}	g/kg	8-20	5.9-18.9	6-26
v_{pdi}	m/s	1-2.5	2-6	1-5
T_{swi}	°C	24.5-40	-	19.3-45
ω_{swi}	g/kg	9.6-20	5.9-18.9	6-26
SPR		1	0.25-2	0.2-0.8
T_{wfi}	°C	-	-	-
$\dot{V}_{wf}$	L/h	-	-	-
T_{pdo}	°C	13.4-28$^{(d)}$	16.1-32.3$^{(a)}$	18.4-31.1$^{(d)}$
T_{swo}	°C	-	-	21.5-44.9$^{(c)}$
ω_{swo}	g/kg	-	-	17-31$^{(a)}$
ε_{wb}		0.25-1.44$^{(a)}$	0.52-1.12$^{(d)}$	0.54-1.29$^{(d)}$
ε_{dp}		0.16-0.94$^{(d)}$	0.36-0.74$^{(d)}$	0.39-0.94$^{(a)}$

Table 10: Summary of selected datasets for the validation of models of D-IEC variations. Unless otherwise specified, all data are directly provided in the reference paper. $^{(a)}$*Data extracted from graph.* $^{(b)}$*Data computed with equations provided in the reference paper.* $^{(c)}$*Data obtained through EB.* $^{(d)}$*Data computed with equations presented in this paper.*

predicted outlet temperature of primary air to the measured temperature reported by Woods and Kozubal [88]. They then extrapolated the behaviour of the evaporative cooler to numerically investigate the effect of inlet air conditions and exchanger geometry on the performance of an M-IEC.

Anisimov et al. [36] numerically compared five EC configurations, including a D-IEC, a perforated D-IEC, a perforated M-IEC, and two crossflow arrangements of the M-IEC. The D-IEC model was validated against the experimental data of Riangvilaikul and Kumar [84]. The accuracy of the mathematical model prediction was then considered to be similar for the perforated D-IEC and M-IEC. Regarding the crossflow M-IECs, they were validated against experimental data obtained with a test bench installed at Coolerado Manufacture, Denver, CO, USA. This study resulted in the creation of two datasets, which allow the validation of multiple evaporative cooler configurations. In the first dataset, various combinations of operational parameters were tested, and data were reported for the primary channel only. In the second dataset, Anisimov et al. provide the evolution profile of the temperature for the primary and secondary airflows and the water film.

Güzelel et al. [35] developed a CFD model of various IEC configurations, including a standard IEC, a D-IEC, a perforated D-IEC, an M-IEC, and a perforated M-IEC. They validated their numerical model against the experimental data of Riangvilaikul and Kumar [84] for the D-IEC configuration. Their study aimed to compare those five configurations in terms of dew point effectiveness, water consumption, and cooling capacity for variable operational conditions. From the dew point effectiveness and water consumption, it was possible to deduce the temperature at the primary outlet and the specific humidity at the secondary outlet. Then, the temperature at the secondary outlet was computed through an energy balance on the evaporative exchanger.

4.5. Two-stage IEC

The datasets for two-stage evaporative coolers reported in this paper are only for two-stage IECs, *i.e.*, the combination of an IEC and a D-IEC in series.

4.5.1. Experimental studies

Chen et al. [89] experimentally studied a crossflow two-stage IEC. The evaporative cooler was designed to operate with only two fans. The IEC and the D-IEC sections are both in a crossflow configuration, such that the outlet secondary air streams are mixed and extracted by a single fan. The evaporative cooler was tested under various air flow rates but constant inlet air conditions. They observed that the two-stage IEC showed better effectiveness than other D-IECs studies in the literature, while working with a lower SPR in the D-IEC section. Only the primary air flow rate and the air flow rate in the D-IEC section were provided in the reference paper. To complete the dataset, it has been assumed that the air velocity was similar in the D-IEC and the IEC sections.

4.5.2. Numerical studies

Pacak et al. [51] developed a numerical model for a two-stage IEC consisting of a D-IEC pre-cooled with a crossflow IEC module, based on the work of Anisimov et al. [59]. Their model was validated for the D-IEC configuration, using two sources of experimental results from the literature. First, the temperature profile of the primary air was validated against the experimental results of Hsu et al. [44]. The model was further validated by comparing the predicted primary air outlet temperature to the measured temperature reported by Lee et al. [90] under various inlet conditions. The numerical model was used to predict the primary air outlet temperature when varying the secondary-to-primary airflow rate ratios and the relative length of both sections of the evaporative cooler.

5. Datasets analysis

This section summarises the main findings resulting from the literature search for datasets. First, the range of inlet conditions for all the considered datasets is analysed. Then, general considerations are given and possible research gaps are identified for each EC type.

Information		Pacak et al. [51]	Chen et al. [89]
		Description	
Method		Num	Exp
Configuration		XF/CF	XF/XF
Water injection		Wet surface	Sprayed water
Dataset size		100	8
		Parameters	
L	m	1	0.44
h_{ch}	mm	3	3
W	m	1	0.4
WWR		1	1
nb_{ch}		185	141
Re		1130-1150$^{(d)}$	190-1460$^{(d)}$
Nu		7.54$^{(d)}$	7.54$^{(d)}$
$h_{T,pd}$	W/m².K	33.4$^{(d)}$	33.6-33.7$^{(d)}$
$h_{T,sw,1}$	W/m².K	33.4$^{(d)}$	33.6-33.7$^{(d)}$
$h_{T,sw,2}$	W/m².K	32.3-32.9$^{(d)}$	32.8-33.1$^{(d)}$
T_{pdi}	°C	30	32.2-32.8$^{(a)}$
ω_{pdi}	g/kg	12	16.6-18$^{(c)}$
v_{pdi}	m/s	3	0.5-4$^{(a)}$
T_{swi}	°C	30	23.7-32.8$^{(a)}$
ω_{swi}	g/kg	12	16.6-18$^{(c)}$
SPR		0.1-1	0.1-0.25
T_{wfi}	°C	-	-
$\dot{V}_{wf}$	L/h	-	-
T_{pdo}	°C	17.8-23.8$^{(a)}$	23.7-26.2$^{(a)}$
T_{swo}	°C	-	-
ω_{swo}	g/kg	-	-
ε_{wb}		0.69-1.36$^{(d)}$	0.83-1.23$^{(a)}$
ε_{dp}		0.47-0.92$^{(d)}$	0.65-0.94$^{(a)}$

Table 11: Summary of selected datasets for the validation of models of 2-stage IECs. Unless otherwise specified, all data are directly provided in the reference paper. $^{(a)}$*Data extracted from graph.* $^{(b)}$*Data computed with equations provided in the reference paper.* $^{(c)}$*Data obtained through EB.* $^{(d)}$*Data computed with equations presented in this paper.*

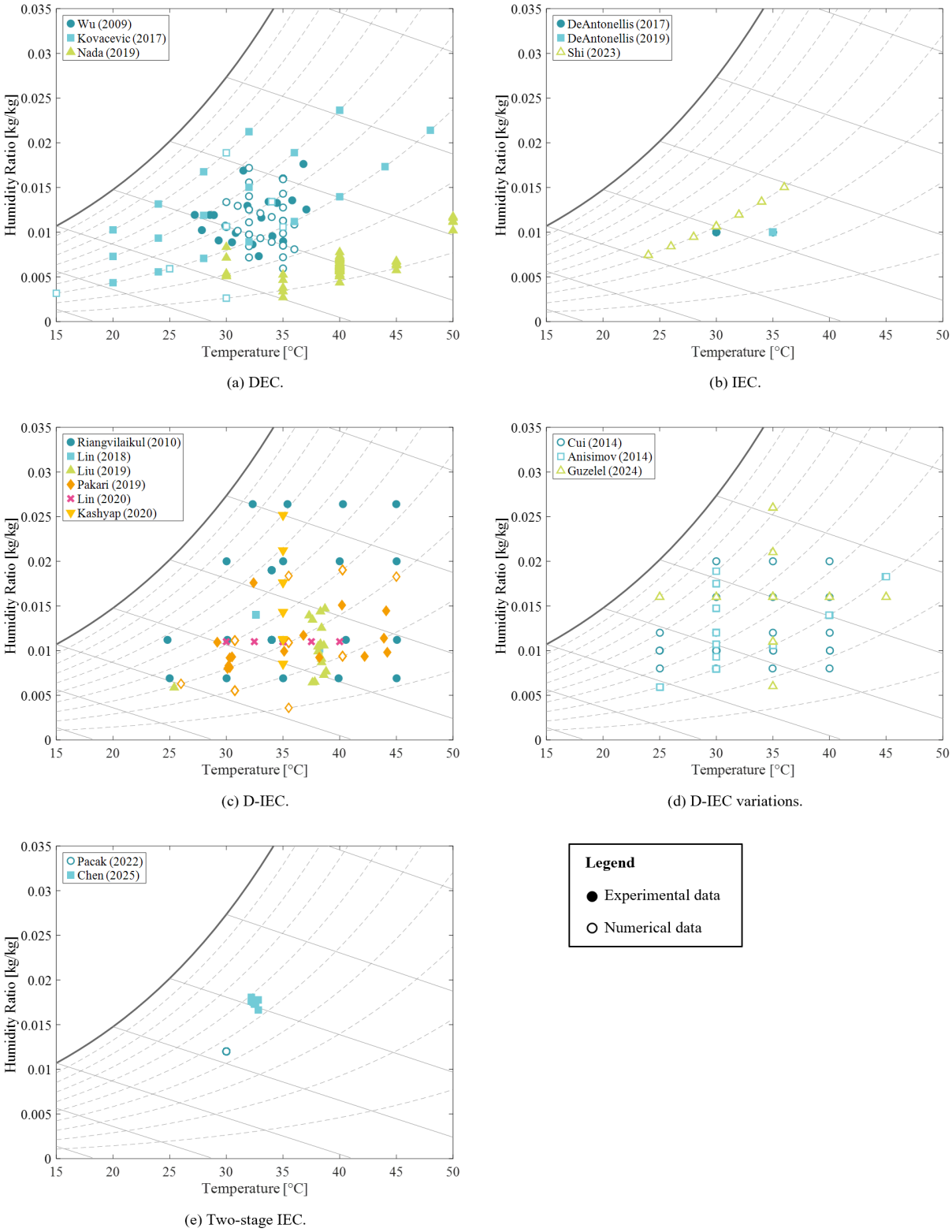

(a) DEC.

(b) IEC.

(c) D-IEC.

(d) D-IEC variations.

(e) Two-stage IEC.

Figure 11: Representation of the tested primary inlet conditions in a psychrometric diagram for all considered EC configurations. The primary inlet conditions cover a large area of the psychrometric diagram.

The tested air conditions at the primary inlet for the studied configurations are summarised in Figure 11. It can be seen that, except for the IEC and the two-stage IEC configurations, the combination of the selected datasets covers a large area of the psychrometric chart, with temperature ranging from 25 to 45°C, and relative humidity from 15 to 80%.

For DECs, three studies were found suitable for results reproduction. The first two studies [45, 79] provide both experimental and numerical data. However, for experimental data, there was no direct measurement of the relative humidity at the exchanger outlet. The specific humidity has been determined based on an energy balance, assuming no heat losses. Moreover, the effect of the water temperature on the DEC performance has not been considered. Nada et al. [80, 81] address these issues by studying the effects of varying the inlet air temperature and velocity, and the water supply temperature and flow rate. However, the specific humidity at the DEC inlet was not directly measured.

For crossflow IECs, De Antonellis et al. [68] provided a dataset that allows performing an energy balance on the heat exchanger, offering an opportunity to validate the model on primary and secondary sides. However, the inlet conditions on the primary side were not varied.

The IEC in counterflow configuration has been studied only numerically. However, it should be noted that if more data are required for the validation of an IEC model, it is possible to use a dataset from the D-IEC configuration. Since the primary air outlet conditions are given in the dataset, they can be used as inlet conditions for the secondary channel.

The D-IEC is the most studied configuration in the literature, in a counterflow arrangement. The combination of the proposed datasets covers a large area on the psychrometric chart regarding inlet conditions. Most studies provide data for the primary air outlet conditions only, which prevents performing an energy balance on the exchanger. Some datasets can also be used to study the effect of the water film temperature [69, 86].

Regarding the other variations of the D-IEC configuration, namely M-IEC, perforated D-IEC and M-IEC, the reported datasets were generated numerically. It is common practice to validate the model based on experimental measurement for the D-IEC configuration only and then to assume the model validity for the other configurations. Two of the selected studies aimed at comparing various IEC configurations, which allows model cross-validation.

The two-stage IEC was studied numerically by Pacak et al. [51], assessing the performance of the two-stage IEC under various operating conditions and geometrical characteristics. Recently, Chen et al. [89] experimentally studied a two-stage IEC for the first time.

A summary of the wet bulb and dew point effectivenesses reported in the selected papers for each EC configuration can be found in Figure 12. The effectiveness spans a wide range of values for most EC configurations. Due to its definition (given in Section 2.5), the effectiveness intrinsically depends on the inlet conditions of temperature and humidity of the primary air. Moreover, the performance of evaporative coolers is impacted by geometric characteristics, secondary-to-primary airflow rate ratio, and inlet air velocity, as it was established in Section 3.1. The effectiveness values presented in this graph cannot be considered universal for each EC configuration; they are provided for information purposes. To accurately compare the various EC configurations using wet bulb or dew point effectiveness, identical tests should be conducted across all configurations. All the parameters influencing the EC performance should be adjusted within a defined range, and a test matrix should be developed to ensure that every possible combination of these parameters is tested. The exchange surface areas should remain consistent for all configurations during the tests, depending on the number of different channels in the considered EC configuration. Once the data set is compiled, conclusions can be drawn regarding the most efficient configurations under given operating conditions.

6. Conclusion and future perspectives

In this work, a new classification for evaporative coolers has been presented. The classification is based on the definition of the channel characteristics, as well as on common variations in the exchanger configuration, namely

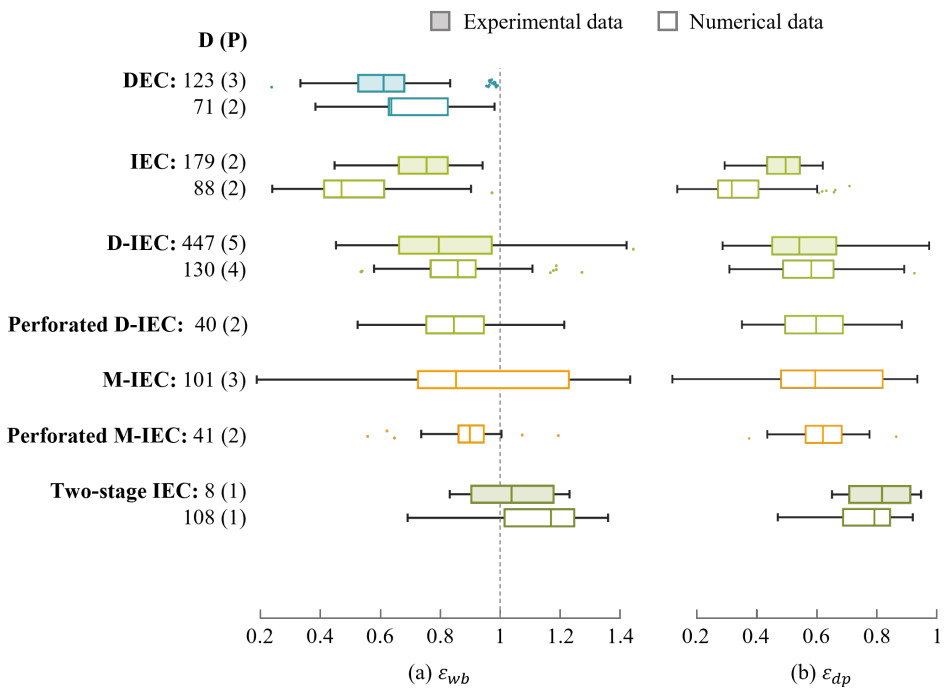

Figure 12: Summary of the wet bulb and dew point effectivenesses reported in the selected papers for each EC configuration. **D** = number of data points, **P** = number of reference papers.

primary air regeneration or perforations between dry and wet channels. For the identified evaporative cooler types, the literature has been searched to find suitable datasets for model validation. Data were extracted from tables and graphs in selected papers and compiled in Excel sheets using the standardised nomenclature presented in this paper. Whenever possible, missing data have been computed based on the energy conservation equation. The aim is to provide exhaustive datasets that can be used for model validation under various exchanger geometries and operating parameters.

A total of 18 datasets have been generated for 7 evaporative cooler configurations. Each dataset is based on the results of a reference paper, including 9 experimental campaigns, 6 numerical investigations, and 3 numerical and experimental studies. Overall, more than 1300 data points are provided to the reader to perform a proper model validation in operating conditions ranging from 25 to 45°C, and 15 to 80% relative humidity.

This paper emphasises experimental shortcomings that could be addressed in future studies, intending to provide complete and exploitable datasets for model validation. All newly generated datasets could then be added to the collaborative online database to facilitate further use and promote open-source research.

- For the DEC configuration, a direct measurement of relative humidity at the heat exchanger outlet would allow checking the energy conservation principle.
- The effect of the water temperature is often neglected in the literature, while it has been shown to impact the performance for the DEC and D-IEC configurations.
- For the IEC configuration, the effect of inlet air conditions on the primary side has not been widely studied. For the reported experimental studies, the inlet conditions of the secondary air have been varied between 30-40°C and 11-13 g/kg, while the primary inlet conditions were kept at a constant humidity ratio of 10 g/kg and a temperature of either 30 or 35°C. In the reported numerical study, the primary inlet temperature was varied in the range 24-36°C at a constant relative humidity of 40%.

- Although the D-IEC configuration is the most studied one, there is currently no study providing data at the inlet and outlet of both primary and secondary sides. Reporting experimental measurement of temperature and humidity at the inlet and outlet of the heat exchanger would allow the reader to apply the energy conservation principle.
- In general, variations of the D-IEC configuration were studied only numerically, as those configurations are uncommon due to certain drawbacks that make them more complicated to use in practice. For example, the M-IEC configuration is less compact than a D-IEC or IEC, and the two-stage cross/counterflow IEC requires three airflows instead of two, implying the need for an additional fan.

Acknowledgement

This work is part of the results of scientific research cooperation between France and Belgium and is supported by the Hubert Curien Programme (PHC TOURNESOL) through the INEScot Project. This work is also a part of the International Energy Agency (IEA) EBC Annex 85 – "Indirect Evaporative Cooling" project activities.

References

[1] European Foundation for the Improvement of Living and Working Conditions., Working conditions and workers' health., Publications Office, LU, 2019.
URL https://data.europa.eu/doi/10.2806/909840

[2] C. Liu, T. Kershaw, D. Fosas, A. Ramallo Gonzalez, S. Natarajan, D. Coley, High resolution mapping of overheating and mortality risk, Building and Environment 122 (2017) 1–14. doi:10.1016/j.buildenv.2017.05.028.
URL https://linkinghub.elsevier.com/retrieve/pii/S0360132317302081

[3] D. F. Birol, The Future of Cooling - Opportunities for energy efficient air conditioning, International Energy Agency.

[4] B. Porumb, P. Ungureşan, L. F. Tutunaru, A. Şerban, M. Bălan, A Review of Indirect Evaporative Cooling Technology, Energy Procedia 85 (2016) 461–471. doi:10.1016/j.egypro.2015.12.228.
URL https://linkinghub.elsevier.com/retrieve/pii/S1876610215028933

[5] E. Elnagar, S. Pezzutto, B. Duplessis, T. Fontenaille, V. Lemort, A comprehensive scouting of space cooling technologies in Europe: Key characteristics and development trends, Renewable and Sustainable Energy Reviews 186 (2023) 113636. doi:10.1016/j.rser.2023.113636.
URL https://linkinghub.elsevier.com/retrieve/pii/S1364032123004938

[6] Y. Cui, J. Zhu, S. Zoras, L. Liu, Review of the recent advances in dew point evaporative cooling technology: 3E (energy, economic and environmental) assessments, Renewable and Sustainable Energy Reviews 148 (2021) 111345. doi:10.1016/j.rser.2021.111345.
URL https://linkinghub.elsevier.com/retrieve/pii/S1364032121006316

[7] M. Santamouris, Urban climate change: reasons, magnitude, impact, and mitigation, in: Urban Climate Change and Heat Islands, Elsevier, 2023, pp. 1–27. doi:10.1016/B978-0-12-818977-1.00002-8.
URL https://linkinghub.elsevier.com/retrieve/pii/B9780128189771000028

[8] L. Lai, X. Wang, G. Kefayati, E. Hu, Evaporative Cooling Integrated with Solid Desiccant Systems: A Review, Energies 14 (18) (2021) 5982. doi:10.3390/en14185982.
URL https://www.mdpi.com/1996-1073/14/18/5982

[9] M. H. Mahmood, M. Sultan, T. Miyazaki, S. Koyama, V. S. Maisotsenko, Overview of the Maisotsenko cycle – A way towards dew point evaporative cooling, Renewable and Sustainable Energy Reviews 66 (2016) 537–555. doi:10.1016/j.rser.2016.08.022.
URL https://linkinghub.elsevier.com/retrieve/pii/S1364032116304361

[10] U. Sajjad, N. Abbas, K. Hamid, S. Abbas, I. Hussain, S. M. Ammar, M. Sultan, H. M. Ali, M. Hussain, Tauseef-ur-Rehman, C. C. Wang, A review of recent advances in indirect evaporative cooling technology, International Communications in Heat and Mass Transfer 122 (2021) 105140. doi:10.1016/j.icheatmasstransfer.2021.105140.
URL https://linkinghub.elsevier.com/retrieve/pii/S0735193321000348

[11] I. Hussain, F. Bibi, S. A. Bhat, U. Sajjad, M. Sultan, H. M. Ali, M. W. Azam, S. K. Kaushal, S. Hussain, W.-M. Yan, Evaluating the parameters affecting the direct and indirect evaporative cooling systems, Engineering Analysis with Boundary Elements 145 (2022) 211–223. doi:10.1016/j.enganabound.2022.09.016.
URL https://linkinghub.elsevier.com/retrieve/pii/S0955799722003186

[12] H. Campaniço, P. Hollmuller, P. M. Soares, Assessing energy savings in cooling demand of buildings using passive cooling systems based on ventilation, Applied Energy 134 (2014) 426–438. doi:10.1016/j.apenergy.2014.08.053.
URL https://linkinghub.elsevier.com/retrieve/pii/S0306261914008642

[13] M. J. Romero-Lara, F. Comino, M. Ruiz de Adana, Seasonal Analysis Comparison of Three Air-Cooling Systems in Terms of Thermal Comfort, Air Quality and Energy Consumption for School Buildings in Mediterranean Climates, Energies 14 (15) (2021) 4436. doi:10.3390/en14154436.
URL https://www.mdpi.com/1996-1073/14/15/4436

[14] Y. E. Güzelel, U. Olmuş, O. Büyükalaca, Simulation of a desiccant air-conditioning system integrated with dew-point indirect evaporative cooler for a school building, Applied Thermal Engineering 217 (2022) 119233. doi:10.1016/j.applthermaleng.2022.119233.
URL https://linkinghub.elsevier.com/retrieve/pii/S1359431122011632
[15] B. Costelloe, D. Finn, Indirect evaporative cooling potential in air–water systems in temperate climates, Energy and Buildings 35 (2003) 573–591.
[16] P. M. Cuce, S. Riffat, A state of the art review of evaporative cooling systems for building applications, Renewable and Sustainable Energy Reviews 54 (2016) 1240–1249. doi:10.1016/j.rser.2015.10.066.
URL https://linkinghub.elsevier.com/retrieve/pii/S1364032115011454
[17] A. De Angelis, O. Saro, M. Truant, Evaporative cooling systems to improve internal comfort in industrial buildings, Energy Procedia 126 (2017) 313–320. doi:10.1016/j.egypro.2017.08.245.
URL https://linkinghub.elsevier.com/retrieve/pii/S1876610217337517
[18] W. Shi, X. Ma, Y. Min, H. Yang, Feasibility Analysis of Indirect Evaporative Cooling System Assisted by Liquid Desiccant for Data Centers in Hot-Humid Regions, Sustainability 16 (5) (2024) 2011. doi:10.3390/su16052011.
URL https://www.mdpi.com/2071-1050/16/5/2011
[19] W. Yan, X. Cui, M. Zhao, X. Meng, C. Yang, Y. Zhang, Y. Liu, L. Jin, Multi-objective optimization of dew point indirect evaporative coolers for data centers, Applied Thermal Engineering 241 (2024) 122425. doi:10.1016/j.applthermaleng.2024.122425.
URL https://linkinghub.elsevier.com/retrieve/pii/S1359431124000930
[20] A. Agrawal, M. Khichar, S. Jain, Transient simulation of wet cooling strategies for a data center in worldwide climate zones, Energy and Buildings 127 (2016) 352–359. doi:10.1016/j.enbuild.2016.06.011.
URL https://linkinghub.elsevier.com/retrieve/pii/S037877881630500X
[21] J. Chu, X. Huang, Research status and development trends of evaporative cooling air-conditioning technology in data centers, Energy and Built Environment 4 (1) (2023) 86–110. doi:10.1016/j.enbenv.2021.08.004.
URL https://linkinghub.elsevier.com/retrieve/pii/S2666123321000544
[22] M. Kashif, H. Niaz, M. Sultan, T. Miyazaki, Y. Feng, M. Usman, M. W. Shahzad, Y. Niaz, M. M. Waqas, I. Ali, Study on Desiccant and Evaporative Cooling Systems for Livestock Thermal Comfort: Theory and Experiments, Energies 13 (11) (2020) 2675. doi:10.3390/en13112675.
URL https://www.mdpi.com/1996-1073/13/11/2675
[23] H. M. U. Raza, M. Sultan, M. Bahrami, A. A. Khan, Experimental investigation of evaporative cooling systems for agricultural storage and livestock air-conditioning in Pakistan, Building Simulation 14 (3) (2021) 617–631. doi:10.1007/s12273-020-0678-2.
URL https://link.springer.com/10.1007/s12273-020-0678-2
[24] F. Kamrani, M. Montazeri, A. Banakar, B. Ghobadian, H. Pasdarshahri, Experimental performance and evaluation of direct evaporative cooling system coupled with a desiccant wheel in a closed greenhouse, Energy Conversion and Management: X 20 (2023) 100497. doi:10.1016/j.ecmx.2023.100497.
URL https://linkinghub.elsevier.com/retrieve/pii/S2590174523001538
[25] C. J. Testa, K. Shvedova, C. Hu, W. Wu, S. C. Born, B. Takizawa, S. Mascia, Heterogeneous Crystallization as a Process Intensification Technology in an Integrated Continuous Manufacturing Process for Pharmaceuticals, Organic Process Research & Development 25 (2) (2021) 225–238. doi:10.1021/acs.oprd.0c00468.
URL https://pubs.acs.org/doi/10.1021/acs.oprd.0c00468
[26] D. Pandelidis, A. Cichoń, A. Pacak, P. Drag, M. Drag, W. Worek, S. Cetin, Water desalination through the dewpoint evaporative system, Energy Conversion and Management 229 (2021) 113757. doi:10.1016/j.enconman.2020.113757.
URL https://linkinghub.elsevier.com/retrieve/pii/S0196890420312802
[27] F. Essa, A. Abdullah, Z. Omara, A. Kabeel, W. M. El-Maghlany, On the different packing materials of humidification–dehumidification thermal desalination techniques – A review, Journal of Cleaner Production 277 (2020) 123468. doi:10.1016/j.jclepro.2020.123468.
URL https://linkinghub.elsevier.com/retrieve/pii/S0959652620335137
[28] R. H. Mohammed, M. El-Morsi, O. Abdelaziz, Indirect evaporative cooling for buildings: A comprehensive patents review, Journal of Building Engineering 50 (2022) 104158. doi:10.1016/j.jobe.2022.104158.
URL https://linkinghub.elsevier.com/retrieve/pii/S2352710222001711
[29] H. Sadighi Dizaji, E. J. Hu, L. Chen, A comprehensive review of the Maisotsenko-cycle based air conditioning systems, Energy 156 (2018) 725–749. doi:10.1016/j.energy.2018.05.086.
URL https://linkinghub.elsevier.com/retrieve/pii/S036054421830906X
[30] H. Yang, W. Shi, Y. Chen, Y. Min, Research development of indirect evaporative cooling technology: An updated review, Renewable and Sustainable Energy Reviews 145 (2021) 111082. doi:10.1016/j.rser.2021.111082.
URL https://linkinghub.elsevier.com/retrieve/pii/S1364032121003701
[31] G. Zhu, T. Wen, Q. Wang, X. Xu, A review of dew-point evaporative cooling: Recent advances and future development, Applied Energy 312 (2022) 118785. doi:10.1016/j.apenergy.2022.118785.
URL https://linkinghub.elsevier.com/retrieve/pii/S0306261922002343
[32] M. S. Alam, M. N. B. Mohd Zubir, M. R. B. Muhamad, S. N. Kazi, H. F. Öztop, S. Abdullah, K. Shaikh, A technological review of dew point evaporative cooling: experimental, analytical, numerical and optimization perspectives, Journal of Building Engineering 91 (2024) 109544. doi:10.1016/j.jobe.2024.109544.
URL https://linkinghub.elsevier.com/retrieve/pii/S2352710224011124
[33] A. M. Zaki, M. H. Bargal, M. A. Antar, E. M. Mokheimer, L. M. Alhems, Advances in indirect evaporative cooling: principles, integrated cycles, economic insights, and environmental implications, Thermal Science and Engineering Progress 67 (2025) 104078. doi:10.1016/j.tsep.2025.104078.
URL https://linkinghub.elsevier.com/retrieve/pii/S2451904925008698
[34] R. Caruana, S. De Antonellis, L. Marocco, M. Guilizzoni, Modeling of Indirect Evaporative Cooling Systems: A Review, Fluids 8 (11)

(2023) 303. doi:10.3390/fluids8110303.
URL https://www.mdpi.com/2311-5521/8/11/303
[35] Y. E. Güzelel, U. Olmuş, O. Büyükalaca, Performance evaluation of different types of indirect evaporative coolers: A CFD-based comparative study, Journal of Building Engineering 96 (2024) 110399. doi:10.1016/j.jobe.2024.110399.
URL https://linkinghub.elsevier.com/retrieve/pii/S2352710224019673
[36] S. Anisimov, D. Pandelidis, J. Danielewicz, Numerical analysis of selected evaporative exchangers with the Maisotsenko cycle, Energy Conversion and Management 88 (2014) 426–441. doi:10.1016/j.enconman.2014.08.055.
URL https://linkinghub.elsevier.com/retrieve/pii/S0196890414007791
[37] S. Abdullah, M. N. B. M. Zubir, M. R. B. Muhamad, K. M. S. Newaz, H. F. Öztop, M. S. Alam, K. Shaikh, Technological development of evaporative cooling systems and its integration with air dehumidification processes: A review, Energy and Buildings 283 (2023) 112805. doi:10.1016/j.enbuild.2023.112805.
URL https://linkinghub.elsevier.com/retrieve/pii/S037877882300035X
[38] V. Vakiloroaya, B. Samali, A. Fakhar, K. Pishghadam, A review of different strategies for HVAC energy saving, Energy Conversion and Management 77 (2014) 738–754. doi:10.1016/j.enconman.2013.10.023.
URL https://linkinghub.elsevier.com/retrieve/pii/S0196890413006584
[39] N. Kapilan, A. M. Isloor, S. Karinka, A comprehensive review on evaporative cooling systems, Results in Engineering 18 (2023) 101059. doi:10.1016/j.rineng.2023.101059.
URL https://linkinghub.elsevier.com/retrieve/pii/S259012302300186X
[40] O. Amer, R. Boukhanouf, H. G. Ibrahim, A Review of Evaporative Cooling Technologies, International Journal of Environmental Science and Development 6 (2) (2015) 111–117. doi:10.7763/IJESD.2015.V6.571.
URL http://www.ijesd.org/index.php?m=content&c=index&a=show&catid=56&id=913
[41] M. Kalsia, A. Sharma, R. Kaushik, Raja Sekhar Dondapati, Evaporative Cooling Technologies: Conceptual Review Study, Evergreen 10 (1) (2023) 421–429. doi:10.5109/6781102.
URL https://hdl.handle.net/2324/6781102
[42] M. G. Haile, R. Garay-Martinez, A. M. Macarulla, Review of Evaporative Cooling Systems for Buildings in Hot and Dry Climates, Buildings 14 (11) (2024) 3504. doi:10.3390/buildings14113504.
URL https://www.mdpi.com/2075-5309/14/11/3504
[43] S. De Antonellis, L. Cignatta, C. Facchini, P. Liberati, Effect of heat exchanger plates geometry on performance of an indirect evaporative cooling system, Applied Thermal Engineering 173 (2020) 115200. doi:10.1016/j.applthermaleng.2020.115200.
URL https://linkinghub.elsevier.com/retrieve/pii/S1359431119351579
[44] S. T. Hsu, Z. Lavan, Optimization of wet-surface heat exchangers, Energy 14 (11) (1989) 757–770.
[45] I. Kovačević, M. Sourbron, The numerical model for direct evaporative cooler, Applied Thermal Engineering 113 (2017) 8–19. doi:10.1016/j.applthermaleng.2016.11.025.
URL https://linkinghub.elsevier.com/retrieve/pii/S1359431116330253
[46] Y. Yang, G. Cui, C. Q. Lan, Developments in evaporative cooling and enhanced evaporative cooling - A review, Renewable and Sustainable Energy Reviews 113 (2019) 109230. doi:10.1016/j.rser.2019.06.037.
URL https://linkinghub.elsevier.com/retrieve/pii/S1364032119304307
[47] H. Sadighi Dizaji, E. J. Hu, L. Chen, S. Pourhedayat, Development and validation of an analytical model for perforated (multi-stage) regenerative M-cycle air cooler, Applied Energy 228 (2018) 2176–2194. doi:10.1016/j.apenergy.2018.07.018.
URL https://linkinghub.elsevier.com/retrieve/pii/S0306261918310456
[48] A. Pacak, W. Worek, Review of Dew Point Evaporative Cooling Technology for Air Conditioning Applications, Applied Sciences 11 (3) (2021) 934. doi:10.3390/app11030934.
URL https://www.mdpi.com/2076-3417/11/3/934
[49] Z. Duan, C. Zhan, X. Zhang, M. Mustafa, X. Zhao, B. Alimohammadisagvand, A. Hasan, Indirect evaporative cooling: Past, present and future potentials, Renewable and Sustainable Energy Reviews 16 (9) (2012) 6823–6850. doi:10.1016/j.rser.2012.07.007.
URL https://linkinghub.elsevier.com/retrieve/pii/S1364032112004480
[50] R. Maurya, D. N. Shrivastav, V. Shrivastava, Performance and Analysis of an Evaporative cooling System : A Review 5 (10) (2014) 9.
[51] A. Pacak, A. Jurga, K. Sierpowski, M. Panek, A. Skołowska, D. Pandelidis, Performance Analysis of the Multi-Stage Dew-Point Indirect Evaporative Air Cooler, Applied Sciences 12 (13) (2022) 6767. doi:10.3390/app12136767.
URL https://www.mdpi.com/2076-3417/12/13/6767
[52] Y. Cengel, A, M. Boles, A, Thermodynamics, An Engineering Approach, 5th Edition, McGraw-Hill, 2006.
[53] F. Bruno, On-site experimental testing of a novel dew point evaporative cooler, Energy and Buildings 43 (12) (2011) 3475–3483. doi:10.1016/j.enbuild.2011.09.013.
URL https://linkinghub.elsevier.com/retrieve/pii/S0378778811004014
[54] X. Cui, K. Chua, M. Islam, K. Ng, Performance evaluation of an indirect pre-cooling evaporative heat exchanger operating in hot and humid climate, Energy Conversion and Management 102 (2015) 140–150. doi:10.1016/j.enconman.2015.02.025.
URL https://linkinghub.elsevier.com/retrieve/pii/S0196890415001387
[55] J. Lin, R. Wang, C. Li, S. Wang, J. Long, K. J. Chua, Towards a thermodynamically favorable dew point evaporative cooler via optimization, Energy Conversion and Management 203 (2020) 112224. doi:10.1016/j.enconman.2019.112224.
URL https://linkinghub.elsevier.com/retrieve/pii/S0196890419312300
[56] G. Zhu, T.-T. Chow, V. S. Maisotsenko, T. Wen, Maisotsenko power cycle technologies: Research, development and future needs, Applied Thermal Engineering 223 (2023) 120023. doi:10.1016/j.applthermaleng.2023.120023.
URL https://linkinghub.elsevier.com/retrieve/pii/S1359431123000522
[57] X. Cui, K. Chua, W. Yang, K. Ng, K. Thu, V. Nguyen, Studying the performance of an improved dew-point evaporative design for cooling application, Applied Thermal Engineering 63 (2) (2014) 624–633. doi:10.1016/j.applthermaleng.2013.11.070.

URL https://linkinghub.elsevier.com/retrieve/pii/S1359431113008740
[58] K. Matsui, K. Thu, T. Miyazaki, A hybrid power cycle using an inverted Brayton cycle with an indirect evaporative device for waste-heat recovery, Applied Thermal Engineering 170 (2020) 115029. doi:10.1016/j.applthermaleng.2020.115029.
URL https://linkinghub.elsevier.com/retrieve/pii/S135943111938408X
[59] S. Anisimov, D. Pandelidis, J. Danielewicz, Numerical study and optimization of the combined indirect evaporative air cooler for air-conditioning systems, Energy 80 (2015) 452–464. doi:10.1016/j.energy.2014.11.086.
URL https://linkinghub.elsevier.com/retrieve/pii/S0360544214013590
[60] D. Pandelidis, S. Anisimov, K. Rajski, E. Brychcy, M. Sidorczyk, Performance comparison of the advanced indirect evaporative air coolers, Energy 135 (2017) 138–152. doi:10.1016/j.energy.2017.06.111.
URL https://linkinghub.elsevier.com/retrieve/pii/S0360544217311088
[61] A. Zeoli, A. Pacak, S. Gendebien, M. Chorowski, X. Xie, V. Lemort, Feasibility Analysis of Desiccant Evaporative Cooling Technologies in Various Climate Conditions: Present and Future Potential, Energy 327 (136257). doi:10.2139/ssrn.5073756.
URL https://www.ssrn.com/abstract=5073756
[62] B. Porumb, P. Ungureşan, L. F. Tutunaru, A. Şerban, M. Bălan, A Review of Indirect Evaporative Cooling Operating Conditions and Performances, Energy Procedia 85 (2016) 452–460. doi:10.1016/j.egypro.2015.12.226.
URL https://linkinghub.elsevier.com/retrieve/pii/S187661021502891X
[63] Cui, Sun, Zhang, Jin, On the Study of a Hybrid Indirect Evaporative Pre-Cooling System for Various Climates, Energies 12 (23) (2019) 4419. doi:10.3390/en12234419.
URL https://www.mdpi.com/1996-1073/12/23/4419
[64] M. Lao, J. Lin, F. Mikšík, K. Thu, T. Miyazaki, Performance and design analyses of various configurations of dew point evaporative cooling-based desiccant air-conditioning (DAC) systems for hot and humid conditions, International Journal of Air-Conditioning and Refrigeration 30 (1) (2022) 12. doi:10.1007/s44189-022-00011-7.
URL https://link.springer.com/10.1007/s44189-022-00011-7
[65] A. Pacak, A. Jurga, B. Kaźmierczak, D. Pandelidis, Experimental verification of the effect of air pre-cooling in dew point evaporative cooler on the performance of a solid desiccant dehumidifier, International Communications in Heat and Mass Transfer 142 (2023) 106651. doi:10.1016/j.icheatmasstransfer.2023.106651.
URL https://linkinghub.elsevier.com/retrieve/pii/S0735193323000404
[66] A. Pacak, A. Cichoń, D. Pandelidis, S. Anisimov, Analysis of the multi-stage desiccant cooling system performance in Wrocław (Poland), E3S Web of Conferences 100 (2019) 00062. doi:10.1051/e3sconf/201910000062.
URL https://www.e3s-conferences.org/10.1051/e3sconf/201910000062
[67] C. Ren, H. Yang, An analytical model for the heat and mass transfer processes in indirect evaporative cooling with parallel/counter flow configurations, International Journal of Heat and Mass Transfer 49 (3-4) (2006) 617–627. doi:10.1016/j.ijheatmasstransfer.2005.08.019.
URL https://linkinghub.elsevier.com/retrieve/pii/S0017931005005430
[68] S. De Antonellis, C. M. Joppolo, P. Liberati, S. Milani, F. Romano, Modeling and experimental study of an indirect evaporative cooler, Energy and Buildings 142 (2017) 147–157. doi:10.1016/j.enbuild.2017.02.057.
URL https://linkinghub.elsevier.com/retrieve/pii/S0378778817306527
[69] S. Kashyap, J. Sarkar, A. Kumar, Comparative performance analysis of different novel regenerative evaporative cooling device topologies, Applied Thermal Engineering 176 (2020) 115474. doi:10.1016/j.applthermaleng.2020.115474.
URL https://linkinghub.elsevier.com/retrieve/pii/S1359431120329562
[70] J. E. Braun, S. A. Klein, J. W. Mitchell, Effectiveness Models for Cooling Towers and Cooling Coils, ASHRAE Transactions 95 (2) (1989) 164–174.
[71] G. Nellis, S. A. Klein, Heat transfer, Cambridge University Press, Cambridge ; New York, 2009, oCLC: ocn228503279.
[72] H. Sadighi Dizaji, E. J. Hu, L. Chen, S. Pourhedayat, Analytical/experimental sensitivity study of key design and operational parameters of perforated Maisotsenko cooler based on novel wet-surface theory, Applied Energy 262 (2020) 114557. doi:10.1016/j.apenergy.2020.114557.
URL https://linkinghub.elsevier.com/retrieve/pii/S0306261920300696
[73] I. L. Maclaine-cross, P. J. Banks, A General Theory of Wet Surface Heat Exchangers and its Application to Regenerate Efaporative Cooling, Journal of Heat Transfer 103 (1981) 579–585.
[74] J. R. Camargo, C. D. Ebinuma, S. Cardoso, A mathematical model for direct evaporative cooling air conditioning system, Engenharia Térmica 4 (2003) 30–34.
[75] A. Fouda, Z. Melikyan, A simplified model for analysis of heat and mass transfer in a direct evaporative cooler, Applied Thermal Engineering 31 (5) (2011) 932–936. doi:10.1016/j.applthermaleng.2010.11.016.
URL https://linkinghub.elsevier.com/retrieve/pii/S1359431110004965
[76] A. Malli, H. R. Seyf, M. Layeghi, S. Sharifian, H. Behravesh, Investigating the performance of cellulosic evaporative cooling pads, Energy Conversion and Management 52 (7) (2011) 2598–2603. doi:10.1016/j.enconman.2010.12.015.
URL https://linkinghub.elsevier.com/retrieve/pii/S0196890410005595
[77] A. Laknizi, M. Mahdaoui, A. Ben Abdellah, K. Anoune, M. Bakhouya, H. Ezbakhe, Performance analysis and optimal parameters of a direct evaporative pad cooling system under the climate conditions of Morocco, Case Studies in Thermal Engineering 13 (2019) 100362. doi:10.1016/j.csite.2018.11.013.
URL https://linkinghub.elsevier.com/retrieve/pii/S2214157X18301138
[78] S. Anbarasu, W. Zuo, Y. Fu, Y. Shukla, R. Rawal, Validated open-source Modelica model of direct evaporative cooler with minimal inputs, Journal of Building Performance Simulation 15 (6) (2022) 757–770. doi:10.1080/19401493.2022.2092652.
URL https://www.tandfonline.com/doi/full/10.1080/19401493.2022.2092652
[79] J. Wu, X. Huang, H. Zhang, Numerical investigation on the heat and mass transfer in a direct evaporative cooler, Applied Thermal Engineering

29 (1) (2009) 195–201. doi:10.1016/j.applthermaleng.2008.02.018.
URL https://linkinghub.elsevier.com/retrieve/pii/S1359431108000938

[80] S. Nada, A. Fouda, M. Mahmoud, H. Elattar, Experimental investigation of energy and exergy performance of a direct evaporative cooler using a new pad type, Energy and Buildings 203 (2019) 109449. doi:10.1016/j.enbuild.2019.109449.
URL https://linkinghub.elsevier.com/retrieve/pii/S0378778819321620

[81] S. Nada, H. Elattar, M. Mahmoud, A. Fouda, Performance enhancement and heat and mass transfer characteristics of direct evaporative building free cooling using corrugated cellulose papers, Energy 211 (2020) 118678. doi:10.1016/j.energy.2020.118678.
URL https://linkinghub.elsevier.com/retrieve/pii/S0360544220317862

[82] S. De Antonellis, C. M. Joppolo, P. Liberati, Performance measurement of a cross-flow indirect evaporative cooler: Effect of water nozzles and airflows arrangement, Energy and Buildings 184 (2019) 114–121. doi:10.1016/j.enbuild.2018.11.049.
URL https://linkinghub.elsevier.com/retrieve/pii/S0378778818323107

[83] W. Shi, H. Yang, X. Ma, X. Liu, A novel indirect evaporative cooler with porous media under dual spraying modes: A comparative analysis from energy, exergy, and environmental perspectives, Journal of Building Engineering 76 (2023) 106874, publisher: Elsevier BV. doi:10.1016/j.jobe.2023.106874.
URL https://linkinghub.elsevier.com/retrieve/pii/S2352710223010537

[84] B. Riangvilaikul, S. Kumar, An experimental study of a novel dew point evaporative cooling system, Energy and Buildings 42 (5) (2010) 637–644. doi:10.1016/j.enbuild.2009.10.034.
URL https://linkinghub.elsevier.com/retrieve/pii/S0378778809002837

[85] J. Lin, D. T. Bui, R. Wang, K. J. Chua, On the fundamental heat and mass transfer analysis of the counter-flow dew point evaporative cooler, Applied Energy 217 (2018) 126–142. doi:10.1016/j.apenergy.2018.02.120.
URL https://linkinghub.elsevier.com/retrieve/pii/S0306261918302514

[86] Y. Liu, Y. G. Akhlaghi, X. Zhao, J. Li, Experimental and numerical investigation of a high-efficiency dew-point evaporative cooler, Energy and Buildings 197 (2019) 120–130. doi:10.1016/j.enbuild.2019.05.038.
URL https://linkinghub.elsevier.com/retrieve/pii/S0378778819304694

[87] A. Pakari, S. Ghani, Regression models for performance prediction of counter flow dew point evaporative cooling systems, Energy Conversion and Management 185 (2019) 562–573. doi:10.1016/j.enconman.2019.02.025.
URL https://linkinghub.elsevier.com/retrieve/pii/S0196890419302079

[88] J. Woods, E. Kozubal, A desiccant-enhanced evaporative air conditioner: Numerical model and experiments, Energy Conversion and Management 65 (2013) 208–220. doi:10.1016/j.enconman.2012.08.007.
URL https://linkinghub.elsevier.com/retrieve/pii/S0196890412003238

[89] Z. Chen, W. Zhao, B. Wang, L. Huang, J. Ding, G. Cheng, D. Bui, A first-of-its-kind two-stage dew-point evaporative cooler with high energy efficiency and compact design, Energy Conversion and Management 341 (2025) 120090. doi:10.1016/j.enconman.2025.120090.
URL https://linkinghub.elsevier.com/retrieve/pii/S0196890425006144

[90] J. Lee, D.-Y. Lee, Experimental study of a counter flow regenerative evaporative cooler with finned channels, International Journal of Heat and Mass Transfer 65 (2013) 173–179. doi:10.1016/j.ijheatmasstransfer.2013.05.069.
URL https://linkinghub.elsevier.com/retrieve/pii/S0017931013004596